HYDRAULIC PROPERTIES OF POROUS MEDIA

by

R. H. Brooks and A. T. Corey

March 1964

3

Several departments at Colorado State University have substantial research and graduate programs oriented to hydrology. These Hydrology Papers are intended to communicate in a fast way the current results of this research to the specialists interested in these activities. The papers will supply most of the background research data and results. Shorter versions will usually be published in the appropriate scientific and professional journals.

federal $ ∴ public domain
not CFR Title 18 protect

HYDRAULIC PROPERTIES OF POROUS MEDIA

by

R. H. Brooks

and

A. T. Corey

HYDROLOGY PAPERS

COLORADO STATE UNIVERSITY

FORT COLLINS, COLORADO

ABSTRACT

Following the Burdine approach, a theory is presented that develops the functional relationships among saturation, pressure difference, and the permeabilities of air and liquid in terms of hydraulic properties of partially saturated porous media. Procedures for determining these hydraulic properties from capillary pressure - desaturation curves are described. Air and liquid permeabilities as a function of saturation and capillary pressure are predicted from the experimentally determined hydraulic properties.

The theory also describes the requirements for similitude between any two flow systems in porous media occupied by two immiscible fluid phases when the nonwetting phase is static and the flow of the wetting phase is described by Darcy's law. The requirements for similitude are expressed in terms of the hydraulic properties of porous media.

TABLE OF CONTENTS

LIST OF FIGURES AND TABLES

e - A subscript meaning "effective".

ϕ - Porosity--the volume of pore space expressed as a fraction of bulk volume of the porous medium--dimensions: none.

ϕ_e - Effective porosity--$\phi(1 - S_r)$--dimensions: none.

h - The elevation of a point in a porous medium above a datum--dimensions: L .

k - Shape factor--a dimensionless parameter which depends on the geometry of pore space but not on size--dimensions: none.

K - The maximum permeability to a particular fluid phase when only one phase occupies the media--dimensions: L^2 . It is sometimes called "intrinsic permeability". With porous media that are stable in the presence of the fluids occupying them, K is a function of the geometry of the media. It is not a function of the viscosity or specific weight of the fluid.

K_e - Effective permeability--the permeability of a porous medium to a particular fluid phase when the medium is occupied by more than one fluid phase--dimensions: L^2 .

K_r - K_e/K

K_x - The component of K in the x-direction--dimensions: L^2 .

L - Length--distance between two points in a porous medium--dimensions: L .

L_e - Effective length--distance traversed by differential fluid elements in moving between two points in a porous medium--dimensions: L .

L_x - Length--the distance between two points in a porous medium in the x-direction--dimensions: L .

R - Hydraulic radius--for tubes of uniform cross section, the cross-sectional area divided by the wetted perimeter. For tubes of non-uniform cross-section, the average hydraulic radius is assumed to be the volume of the tube divided by its internal surface area--dimensions: L .

nw - A subscript meaning "non-wetting phase". A non-wetting fluid phase is a fluid that does not directly contact the solid surfaces in the presence of another fluid which wets the surface. In an air-water system, for example, water is usually the wetting and air the non-wetting phase.

P - Pressure--usually a measure of the compressive force of fluid at a point and in the case of a static fluid it usually is the average intensity of the surface force acting on the fluid element as a point. In the case of a wetting fluid in porous media where adsorptive forces act, the meaning is expanded to the quantity which is measured by a tensiometer at atmospheric pressure--dimensions: FL^{-2} .

P* - Piezometric pressure--the quantity $P + \gamma h$.--dimensions: FL^{-2} .

P_b - Bubbling pressure--approximately the minimum P_c on the drainage cycle at which a continuous non-wetting phase exists in a porous medium. For a more rigorous definition see section on experimental methods--dimensions: FL^{-2} .

P_c - Capillary pressure--the pressure difference $(P_{nw} - P_w)$--dimensions: FL^{-2} .

q - Volume flux--the maximum component of the volume rate of discharge of a flowing fluid per unit area of the bulk medium. In an isotropic medium the area referred to is a cross-section perpendicular to the potential gradient producing the flow--dimensions: LT^{-1} .

q_x - Component of q in the x-direction--dimensions: LT^{-1} .

r - A radial distance--dimension: L--also a subscript meaning "ratio" or "residual".

S - Saturation--the ratio of the volume of wetting fluid to the volume of interconnected pore space in a bulk element of the medium--dimensions: none .

S_e - Effective saturation--given by $(S - S_r)/(1 - S_r)$--dimensions: none.

S_r - The residual saturation--a saturation at which the theory assumes that K_{ew} is zero and K_{enw} is a maximum. The method of determining S_r is given in Appendix II.

T - Tortuosity--the ratio $(L_e/L)^2$--dimensions: none.

u - A component of fluid velocity in the direction x--dimensions: LT^{-1} .

$\bar{u}$ - Mean value of u --the average value of u over a cross-section of fluid perpendicular to x--dimensions: LT^{-1} .

$\underline{V}$ - The total velocity vector--the vector sum of u, v, and w the components of fluid velocity in the x, y, and z coordinate directions respectively--dimensions: LT^{-1} .

v - Volume--dimensions: L^3 .

w - A subscript meaning wetting phase. A fluid that wets the solid surfaces of the media. In an air-water system, water is the wetting phase.

γ - Specific weight of fluid--weight per unit volume of fluid--dimensions: FL^{-3} .

Δ - Denotes a difference.

∇ - Denotes the gradient operator.

$\nabla.$ - Denotes the gradient operator with respect to scaled coordinate distances.

div - Denotes the divergence operator.

Div. - Denotes the divergence operator with respect to scaled coordinate distances.

ϵ - The exponent in the equation: $K_{rw} = S_e^{\epsilon}$.

η - The exponent in the equation: $K_{rw} = (P_b/P_c)^{\eta}$.

λ - The exponent in the equation: $S_e = (P_b/P_c)^{\lambda}$, called the pore-size distribution index.

μ - Dynamic viscosity--dimensions: FL^2T^{-1} .

μ^2 - Square microns--a unit of permeability--dimensions: L^2 .

σ - Interfacial tension--dimensions: FL^{-1} .

HYDRAULIC PROPERTIES OF POROUS MEDIA[1]

R. H. Brooks and A. T. Corey[2]

INTRODUCTION

Irrigation and drainage engineers are faced with the problem of getting water into or out of soil. In either case, the flow phenomenon involved is flow through partially saturated porous media. When water enters a soil, air must be replaced; and when water is removed, air must enter. The flow, therefore, involves two largely immiscible fluids: air and water.

Most of the literature describing flow of two immiscible fluids is found in journals concerned with petroleum technology or with soil physics. Because the language in some of the literature is unfamiliar and because much of it is qualitative in nature, drainage and irrigation engineers have not made use of the available information concerning two-phase flow. In the design of drainage and irrigation systems, engineers (with rare exceptions) have made the simplifying assumptions that soil is either completely saturated with water or it is completely unsaturated and that resistance to flow of air (associated with the movement of water into and out of soil) is negligible. Such assumptions are in most cases far from realistic. In real cases, there exist functional relationships among the saturation, the pressure difference between air and water, and the permeabilities of air and water. The purpose of this paper is to describe these functional relationships and the properties of porous media which affect them. The experimental evidence presented indicates that these functional relationships (for isotropic media) can be described in terms of two pertinent soil parameters. One of these parameters is called the "bubbling pressure" which is related to the maximum pore-size forming a continuous network of flow channels within the medium. The other parameter is called the "pore-size distribution index" which evaluates the distribution of sizes of the flow channels within a particular porous medium.

Theory is presented which develops the functional relationships among saturation, the pressure difference, and the permeabilities of air and water in terms of the bubbling pressure and the distribution index. The theory also describes the requirements for similitude between any two flow systems in porous media occupied by two immiscible fluid phases when the nonwetting phase is static and the flow of the wetting phase is described by Darcy's law. The requirements for similitude are also expressed in terms of the bubbling pressure and the pore-size distribution index.

Methods of measuring the bubbling pressure and the pore-size distribution index are presented, and the problem of selecting suitable porous media for use in laboratory models is discussed.

In the two-fluid system discussed herein, the fluids are assumed to be immiscible. They are referred to as the nonwetting and wetting phases. Even though the discussion is confined to a gas-liquid system, the theory applies to any two-fluid system in which the fluids are immiscible.

A convenient way to determine which phase is the wetting phase is to consider the two fluids in a capillary tube. At the interface of the two fluids, the curvature is always concave toward the wetting fluid. For example, in a mercury-air system, the air is the wetting phase; whereas in an air-water system, the air is the nonwetting phase. In the experiments conducted for this paper the two fluids were air and oil.

It is assumed that Darcy's equation applies to flow of both the gas and liquid phases occupying a porous medium. For this assumption to be valid, both phases must form continuous networks within the medium and any isolated bubbles of gas must be regarded as part of the porous matrix. Darcy's equation is written as

$$q_x = -\frac{K_x}{\mu}\left[\frac{\Delta P}{L_x} + \frac{\gamma \Delta h}{L_x}\right] \tag{1}$$

in which q_x is the component of volume flux in the x-direction, γ is the specific weight of the fluid, μ is the viscosity, Δh and ΔP are the difference in elevation and pressure respectively over the distance L_x in the x-direction, and K_x is the permeability in the x-direction. The volume flux q_x is the volume of fluid (liquid or gas) passing a unit cross-sectional area of the porous medium perpendicular to the x-direction in a unit of time. The permeability K_x has dimensions of length squared and it is sometimes called "intrinsic permeability". For a stable, homogeneous, isotropic medium with pores containing only one fluid, permeability is a constant and is considered a property of the medium.

When two immiscible fluids occupy the pores of a porous matrix, the permeability to one fluid phase is called "effective permeability," K_e. For a homogeneous isotropic medium containing a fluid of constant and uniform density,

$$q = -\frac{K_e}{\mu} \nabla P* \tag{2}$$

where q is the largest component of flux (which is in the direction of $\nabla P*$ and $P*$ is the quantity $P + \gamma h$. In general, the effective permeability will depend on the fraction of the total pore space occupied by one fluid phase. The subscript e to the coefficient K indicates that the permeability is not necessarily that of a medium occupied by only one fluid. Usually the effective permeability will be smaller than K, the permeability when only one fluid occupies the medium. The ratio K_e/K is called "relative permeability" and varies from 0 to 1.0. The fraction of the total pore space occupied by the wetting phase is defined as saturation S. It is considered here as a quantity which can vary from point to point within the medium. It is given by the relation

$$S = \frac{\Delta v \text{ (fluid)}}{\Delta v \text{ (pores)}} \tag{3}$$

where Δv (fluid) is the volume of fluid occupying a portion of the pore volume, Δv (pores), of a small volume element, ΔV, of the medium.

In general, the functional relationship, $K_e = f(S)$, is not single-valued but is affected by hysteresis. The value of K_e will be different if a given value of S is obtained by starting with a dry medium and increasing the liquid saturation than if the same value of S is obtained by removing liquid from an initially vacuum-saturated medium. Hysteresis affects both the liquid and the gas permeabilities.

Another assumption of this analysis is that the liquid and gaseous fluid phases are separated by curved interfaces, concave with respect to the liquid. This assumption is valid at relatively high liquid saturations in a medium containing at least some pores large enough that the liquid permeability is substantial. It is not always valid for saturations less than field capacity or for porous media having only extremely small pores, e.g., the spaces between clay platelets.

When liquid is separated from a gas by an interface, a pressure difference exists across the interface. This pressure difference is called capillary pressure P_c and is related to the interfacial tension and curvature of the interface by the equation

$$P_c = \sigma\left[\frac{1}{r_1} + \frac{1}{r_2}\right] = P_{gas} - P_{liquid} \tag{4}$$

where σ is the interfacial tension, r_1 and r_2 are major and minor radii of curvatures at a point on the interface. In all cases considered here, the solid matrix is wet by the liquid so that the liquid (except that in films under the influence of adsorptive forces) is at a pressure less than the pressure of the gas, and P_c is, therefore, positive.

The value of P_c depends on saturation and on the geometry of the pore space in which the interface occurs, being larger in small spaces than in large spaces for a given saturation. When a gas displaces a liquid from a porous medium (by gradually increasing P_c), the first liquid displaced is that occupying the largest pores in contact with the gas. As P_c is increased further, the interfaces retreat to successively smaller spaces. The saturation is, therefore, a function of P_c, and K_e is also a function of P_c, both being affected by hysteresis.

This paper is concerned primarily with desorption or drainage of liquid from media, thereby avoiding the hysteresis problem. However, a short discussion is presented at the end of the paper on the subject of hysteresis.

If engineers are to deal with the flow of water above the water table in connection with either irrigation or drainage of soils, a knowledge of the func-

tional relationship among effective permeability, saturation and capillary pressure is essential. This paper develops these functional relationships using a model of porous media developed by investigators [3, 4, 11, 19] in the petroleum industry. Specifically, the analysis presented here is an extension of the work of Burdine [3].

According to the analysis of Burdine, the relative permeability, K_e/K_w, is approximated by the relation:

$$K_{rw} = \left(\frac{S - S_r}{1 - S_r}\right)^2 \frac{\int_0^S \frac{dS}{P_c^2}}{\int_0^1 \frac{dS}{P_c^2}} \qquad (5)$$

where S_r is the residual saturation, sometimes called irreducible saturation in the petroleum literature. The permeability is assumed to approach zero at this finite saturation. Corey called the quantity $(S - S_r)/(1 - S_r)$ the effective saturation, S_e. By making a change of variable from S to S_e in the integrals of the above equation, the relative wetting phase permeability becomes

$$K_{rw} = (S_e)^2 \frac{\int_0^{S_e} \frac{dS_e}{P_c^2}}{\int_0^1 \frac{dS_e}{P_c^2}} . \qquad (6)$$

Similarly, for the nonwetting phase

$$K_{rnw} = (1 - S_e)^2 \frac{\int_{S_e}^1 \frac{dS_e}{P_c^2}}{\int_0^1 \frac{dS_e}{P_c^2}} . \qquad (7)$$

For the details of the Burdine development leading up to equations (6) and (7), the reader is referred to Appendix I. The ratio of integrals given in equations (6) and (7) can be evaluated graphically or numerically. It can also be evaluated analytically, if a suitable algebraic expression for $S_e = f(P_c)$ can be written.

Corey [5] found that for a large number of consolidated porous rock, the ratio of integrals on the right of equations (6) and (7) is approximately equal to S_e^2 and $(1 - S_e)^2$ respectively. He therefore proposed (as a convenient approximation) the equations:

$$K_{rw} \approx S_e^4 , \qquad (8)$$

$$K_{rnw} \approx (1 - S_e)^2 (1 - S_e^2) . \qquad (9)$$

The approximate equations of Corey have considerable utility because the only parameter needed

for their solution is the residual saturation. Because of their convenience, the equations of Corey are often used in the petroleum industry for making engineering calculations in regard to solution-gas drive petroleum reservoirs. A comparison of their validity and convenience with respect to other methods of estimating K_{rw} was made by Loomis and Crowell [12].

The approximations given by Corey imply that effective saturation, S_e, is a linear function of $1/P_c^2$, i.e.

$$S_e = \left(\frac{c}{P_c}\right)^2 \text{ for } P_c \geq c \qquad (10)$$

where c is some constant. For most porous media, equation (10) is not strictly correct. The authors have plotted several hundred capillary pressure-desaturation curves using data from consolidated rock samples and found only a few samples in which the linear relationship was essentially true. However, when Corey's approximations were compared with experimental data of K_{rw} and S_e from some of these same rock samples, the comparison was favorable. Evidently, the relative permeabilities as a function of S_e are not very sensitive to changes in the actual shape of the capillary pressure curve.

According to equation (6) for a completely uniform pore-size distribution, the value of the exponent in Corey's equation (8) would be 3.0. Averjanov [1] and Irmay [8] proposed equations similar to equation (8) in which values of 3.5 and 3.0 respectively were used as the exponent in their equations. Both of these investigators applied their equations to unconsolidated sands having a single-grain structure. Evidently, unconsolidated sands have a narrow range of pore sizes that are not absolutely uniform but which are more nearly uniform than most soils or consolidated rocks.

Theoretically, Corey's approximations are valid only for a particular pore-size distribution. If equation (10) is substituted into equation (8), the result is

$$K_{rw} = \left(\frac{c}{P_c}\right)^8 , \qquad (11)$$

but for media with relatively uniform pores the exponent in equation (11) is much larger than 8 and theoretically could increase without bound. Evidently, permeability is a very sensitive function of capillary pressure. Obviously, equation (11) cannot be valid for all porous media because permeability and saturation are not unique functions of capillary pressure, as Corey's equations imply, but depend upon the size and arrangement of the pores. Thus, a general relationship between saturation and capillary pressure is needed that will apply to a wide range of media. Such a relationship will allow equations (6) and (7) to be integrated and provide general relationships among the variables (permeability, saturation, and capillary pressure) for both the wetting and nonwetting phases. If the relationships among the variables can be shown to agree with experimental data, the Burdine approach will be greatly strengthened. Also, permeability can be predicted not only as a function of saturation but as a function of capillary pressure as well.

3

The basis for the theory of this section is the observation from a large number of experimental data that

$$S_e = \left(\frac{P_b}{P_c}\right)^\lambda \quad \text{for } P_c \geq P_b \qquad (12)$$

where λ and P_b are characteristic constants of the medium. It will be shown later that λ is a number which characterizes the pore-size distribution and P_b is a measure of the maximum pore-size forming a continuous network of flow channels within the medium.

Equation (12) was discovered by plotting log S_e as a function of log P_c/γ on the drainage cycle. The result (for all media investigated to date) is a straight line with a negative slope λ for $P_c/\gamma \geq P_b/\gamma$. Figure 2 shows examples of this kind of plot for several media. The parameter P_b/γ is defined by the intercept where the straight line meets the ordinate representing $S_e = 1.0$ and it is called the bubbling pressure of the medium.

To determine S_e for the particular values of P_c/γ, it is necessary to have precise capillary pressure desaturation data such as that shown in figure 1. Also, the residual saturation S_r must be known to compute S_e. The procedure for determining S_r is explained in detail in Appendix II. For the purpose of this paper, the definition of residual saturation is implicit in the method of its determination, but it is roughly analogous to the non-drainable water content referred to by drainage engineers. The negative of the slope of the curve of S_e as a function of P_c/γ is designated as λ, and it is called the pore-size distribution index of the medium.

If equation (12) is substituted into equation (6) and the indicated integrations are performed, the relative permeability of the wetting phase becomes

$$K_{rw} = (S_e)^{\frac{2 + 3\lambda}{\lambda}} = (S_e)^\epsilon \qquad (13)$$

or

$$K_{rw} = \left(\frac{P_b}{P_c}\right)^\eta \quad \text{for } P_c \geq P_b \qquad (14)$$

where $\eta = 2 + 3\lambda$ and $\epsilon = (2 + 3\lambda)/\lambda$.

Similarly, for the nonwetting phase

$$K_{rnw} = (1 - S_e)^2 \left(1 - S_e^{\frac{2 + \lambda}{\lambda}}\right) \qquad (15)$$

or

$$K_{rnw} = \left[1 - \left(\frac{P_b}{P_c}\right)^\lambda\right]^2 \left[1 - \left(\frac{P_b}{P_c}\right)^{2 + \lambda}\right] \qquad (16)$$

for $P_c \geq P_b$.

Equations (12) - (16) present the theory regarding the interrelationships among the variables P_c, S_e, K_{rw}, and K_{rnw}. By experimentally determining the parameters P_b, λ, and K, the effective permeabilities to either the wetting or nonwetting fluid phase at any effective saturation or capillary pressure may be predicted.

It is expected that this theory is valid only for isotropic media and possibly only for the drainage cycle. It should, however, be valid for any pore-size distribution since equation (12) has been found to hold for media having a wide range of pore-size distributions.

Theoretically, λ could have any positive value greater than zero, being small for media having a wide range of pore sizes and large for media with a relatively uniform pore size. It seems logical, therefore, to designate the exponent λ as the pore-size distribution index.

Equations (13) and (14) have been expressed in terms of the exponents ϵ and η as it is possible to determine these exponents experimentally without any knowledge of the capillary pressure desaturation curve. It is interesting to note that if the lower limit of λ is zero, the theoretical lower limit of η is 2.

In applying this theory, it should be recognized that values of S_e and K_{ew} may exist at $P_c < P_b$, but the theory does not hold for $P_c < P_b$. The significance of the parameter P_b is discussed in more detail in the following sections. It should also be recognized that values of $S < S_r$ can exist but that the theory cannot apply in this range of saturations and may become inaccurate at saturations very close to S_r.

The theory makes the simplifying assumptions that K_{ew} is zero and K_{enw} is a maximum at S_r. Neither is actually true. It is a fact, however, that when the curves of K_{ew} as a function of S are extrapolated, K_{ew} appears to approach zero at the finite saturation S_r.

Still another limitation of the theory is that it assumes that the porous matrix will not undergo any change in geometry as it changes from a full saturated condition to a value of S approaching S_r.
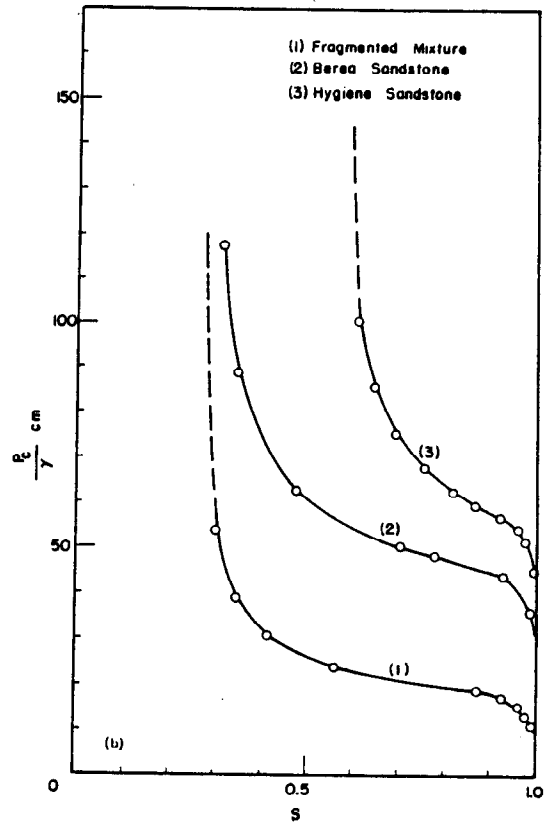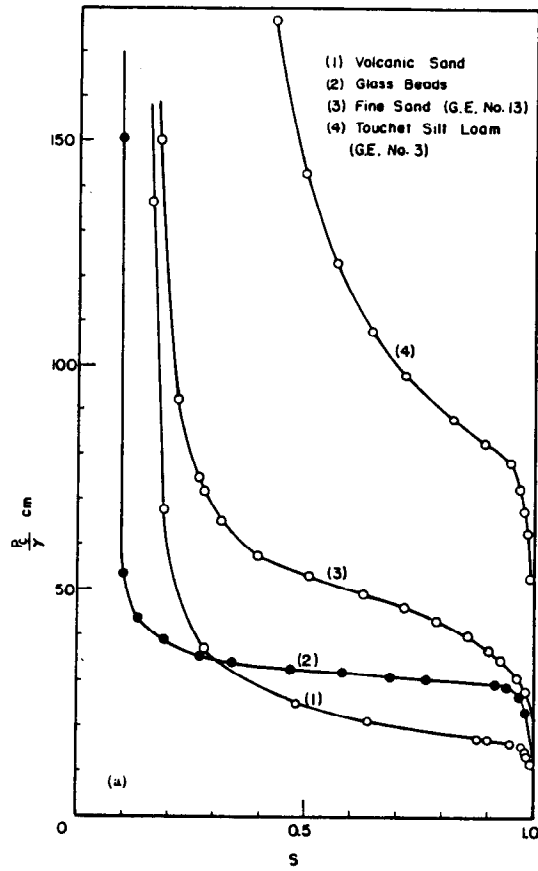
Figure 1. Capillary pressure head as a function of saturation for
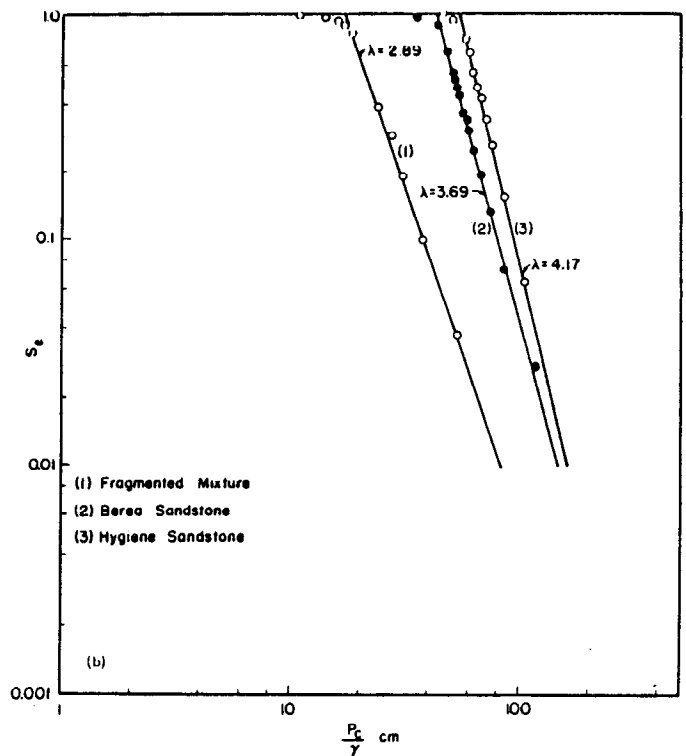porous materials of varying pore-size distributions.
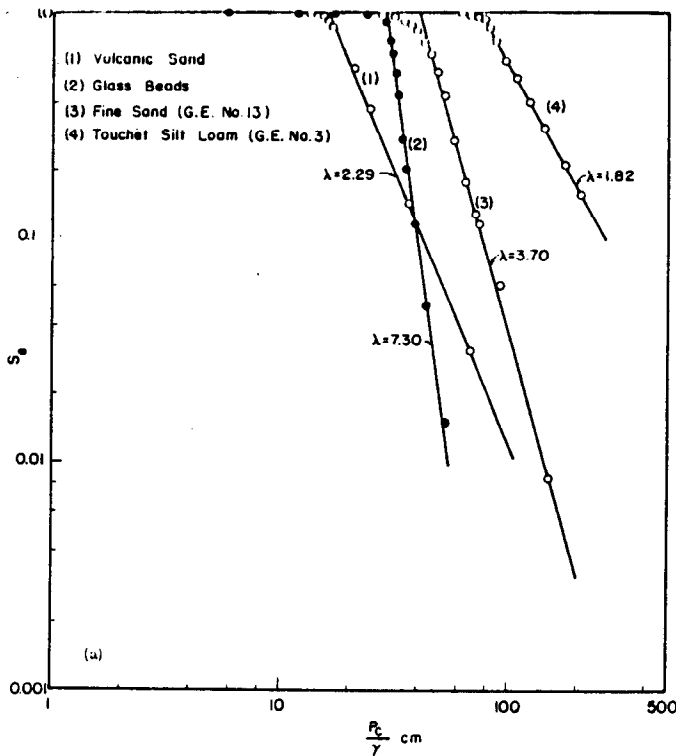

Figure 2. Effective saturation as a function of capillary pressure head
for porous materials of varying pore-size distributions.

5

To date, the authors have investigated mostly unconsolidated media in verifying the theory because it has been easier to create unconsolidated media which are isotropic than to find consolidated porous rocks which are isotropic. The authors have developed ways to measure S, P_c, and K_{enw} simultaneously with sufficient precision on the unconsolidated samples. To date, it has been necessary to measure K_{ew} as a function of P_c by separate experiments, because methods of measuring K_{ew} and K_{enw} simultaneously with sufficient precision for unconsolidated media have not yet been developed. One method that has been described in the literature by Corey [6] results in defective measurements of K_{enw} in the high saturation (low K_{enw}) range.

Precise curves of S as a function of P_c were obtained with a device such that the entire sample was held at a uniform capillary pressure from top to bottom. Ordinarily in a liquid-gas system, the difference in specific weight of the two fluids will produce a greater P_c at the top of a sample than at the bottom (under static conditions).

To overcome this difficulty, all the curves for unconsolidated media shown in figure 1 were determined by maintaining a pressure difference in the air phase exactly equal to the difference in the static liquid pressure between the top and bottom of the sample. It was convenient to measure the gas permeability simultaneously by measuring the flow of air that resulted from the greater air pressure at the bottom of the sample. The flow diagram is presented in figure 3 and the cell used for containing the unconsolidated sample is shown in figure 4.

By-passing of air along the boundaries was prevented by providing a rubber sleeve which was held against the outer circumference of the sample with a pneumatic pressure from 5 - 20 psi depending upon the texture of the sample. Liquid was removed through a hollow ceramic cylinder which was filled with liquid and connected to a calibrated glass tube for measuring the outflow. The media samples occupied the annular space between the hollow ceramic cylinder and the rubber sleeve.

A pair of pressure control reservoirs controlled the liquid pressure in the medium. A flexible plastic tube connected the top of the upper reservoir to the outflow end of the horizontal measuring tube. Another flexible plastic tube connected the bottom of the upper reservoir to the bottom of the lower reservoir, the top of the lower reservoir being open to the atmosphere. The liquid pressure in the medium was decreased in increments by lowering the lower reservoir, the pressure being measured with respect to atmospheric pressure by the difference in liquid elevations in the upper and lower reservoirs at equilibrium. A correction was made for the capillarity of the outflow measuring tube and for its position relative to the sample container.

The capillary pressure was determined by the difference in pressure between the air and the liquid in the medium. The saturations of the samples were determined by noting the accumulated outflow from the medium at each increment of capillary pressure (after outflow stopped) and subtracting this from the total liquid contained in the fully saturated samples.

The pressure of the air at the bottom of the samples was maintained greater than atmospheric by an amount equal to the static liquid pressure difference between the bottom and top of the samples. The air pressure at the bottom of the samples was controlled by a precision pressure regulator, the air pressure at the top of the samples being atmospheric.

The resulting upward flow of air was measured with one of several soap-film flowmeters of different sizes, depending on the amount of discharge. These flowmeters measure the volume flux directly and require no calibration other than the initial calibration of the tube containing the soap film. The calibrated soap-film tubes are encased in evacuated and sealed glass shells so that temperature fluctuations in the room had little affect on the measurements.

In order to prevent errors in measurement of saturation due to liquid being removed as vapor in the flowing air, the air entering the media was presaturated with the vapor of the liquid used in the medium.

Measurement of liquid relative permeability as a function of capillary pressure was accomplished in separate experiments using an apparatus similar to that employed by Scott and Corey [18]. The columns varied in length and were considerably shorter than those employed by Scott and Corey in order that they could be packed in a homogeneous and reproducible manner using a mechanical packer patterned after a design by Jackson et. al. [9]. In one case (the granulated mixture) the column was packed by a method similar to that suggested by Reeve and Brooks [16].

The column method permits steady downward flow with the wetting phase at practically constant pressure along the length of the test section of the columns. The capillary pressure was, therefore, nearly constant during a particular measurement. A series of tensiometer rings sensed the pressure by contact around the circumference of the columns and did not interfere in any way with the flow section.

The columns were first vacuum saturated. The maximum wetting phase permeability was then determined by downward flow at a pressure slightly less than the pressure of the surrounding air, but not enough less to permit air to invade the columns. The capillary pressure was then increased in increments by decreasing the pressure of the wetting fluid at the top and bottom of the columns. This was possible because the wetting fluid entered and left the columns through porous barriers that remained completely saturated throughout the experiments.

When P_c was increased beyond a critical value, air penetrated the columns through joints in the plastic walls of the columns. After the penetration of air stopped and the flow reached a steady state as
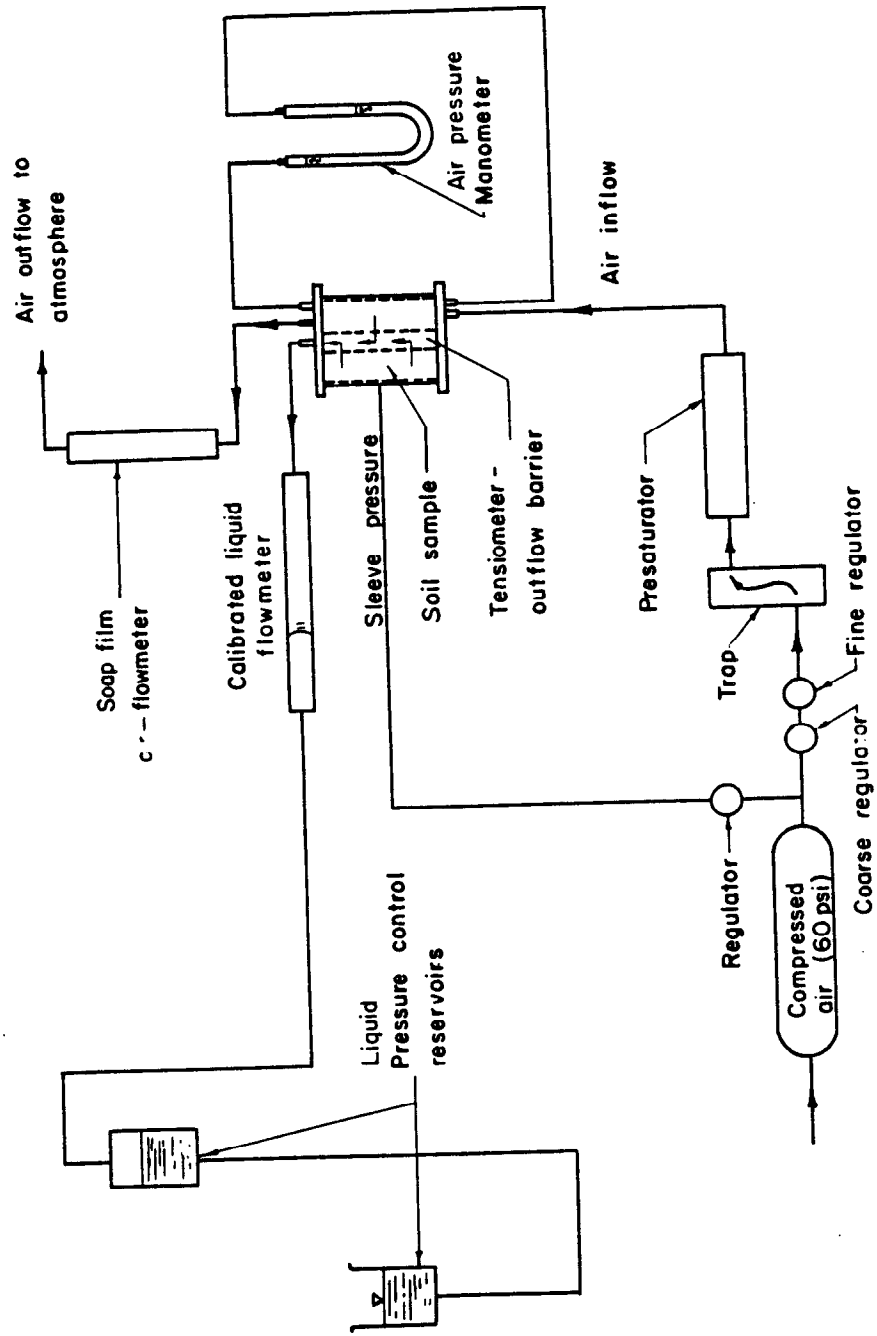
Figure 3. Diagram of flow system and pressure control system for air permeability cell.
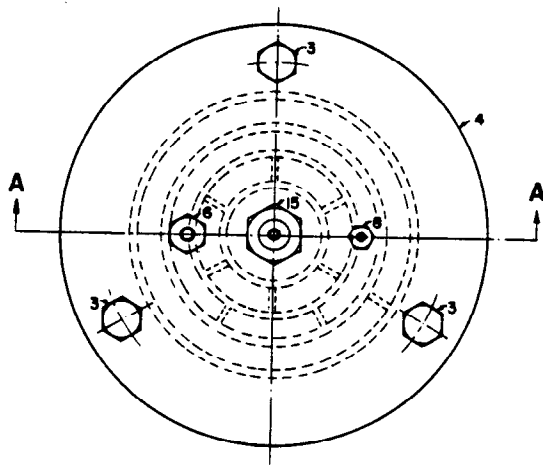
TOP VIEW
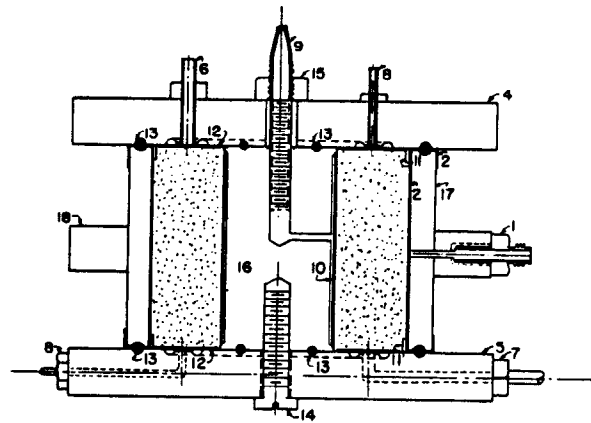
SECTION A-A

FRONT VIEW

Part No.	Name	Size	No. req'd	Material
1.	Sleeve Pressure Tap	1/8" tube--1/8" MPT	1	Brass (Swagelok)
2.	Rubber Sleeve	2-1/2 ID x 1/32" wall x 4"	1	Hycar tubing, Durometer 35
3.	Head Bolt	1/4"-20 x 2-1/2"	6	Steel
4.	Upper Head Plate	4-3/4" dia. x 1/2" thick	1	Plastic
5.	Lower Head Plate	4-3/4" dia. x 1/2" thick	1	Plastic
6.	Air Outflow Tap	1/4" tube-1/4" - 28 M.T.	1	Brass
7.	Air Inflow Tap	1/4" tube-1/4" - 28 M.T.	1	Brass
8.	Manometer Tap	1/8" tube--5-40 M.T.	2	Brass
9.	Liquid Outflow Tap	3/16" tube-3/8"-16 M.T.	1	Steel (air tight connection with Part 16)
10.	Ceramic Barrier to Air	3.25 cm. OD x 1.5 mm wall x 5.5 cm.	1	Ceramic (Selas 015) bubbling pressure = 15 PSI
11.	Retainer Ring	6.8 cm. OD x 0.5 mm wall x 0.4 cm.	2	Steel
12.	Fiber Glass Disk	7.0 cm. dia. x 0.6 mm	2	Fiberglass
13.	O Ring	2-7/8"ID x 1/8" wall 11/16" ID x 3/32" wall	2 2	Neoprene Neoprene
14.	Lower Tensiometer Screw	1/4"-20 x 1"	1	Brass
15.	Upper Tensiometer Nut	3/8"-16 NC	1	Brass
16.	Tensiometer-liquid Outflow Assembly	3.25 cm. OD x 5.5 cm.	1	Plastic and Ceramic
17.	Sleeve Cylinder	2-3/4" ID x 1/4" wall x 2-1/8"	1	Plastic
18.	Head Bolt Ring	4-3/4" OD x 2-3/4" ID x 1/2"	1	Plastic (cemented to Part 17)
19.	Head Bolt Spacer	3/8" OD x 1/16" wall x 1/2"	6	Steel tube

MPT = Male pipe thread
MT = Male thread

Figure 4. Construction details of air permeability cell.

indicated by the steadiness of the discharge and the readings from manometers attached to the tensiometer rings, the discharge was measured and the effective permeability determined. The process was repeated over the desired range of P_c.

In order to compare the nonwetting phase permeabilities with the wetting phase permeabilities, the air permeability cell was packed with a medium at a porosity as near as possible to that obtained with the same material with the column packer. The columns used for the wetting phase permeability measurements, however, did not have a pressurized sleeve. In one case, with a silt loam soil, the air permeameter cell with its pressurized sleeve caused the medium to compress to a final porosity substantially less than that obtained with the column packer. This would probably happen with any highly compressible soil when it is saturated. In the case of the granular materials used in this investigation, it was usually possible to obtain nearly the same porosities in the air permeameter cell as in the sleeveless columns.

In all cases the wetting fluid was a hydrocarbon liquid* and the nonwetting fluid was air. The hydrocarbon was selected instead of water primarily because soil structure is much more stable in the presence of the hydrocarbon than in the presence of water. The hydrocarbon also has more consistent wetting properties, and its surface tension is not changed as readily by contaminants. The relationship between the capillary pressure head for water and oil in a stable medium was experimentally found to be

$$\left(\frac{P_c}{\gamma}\right)_w \approx 2\left(\frac{P_c}{\gamma}\right)_o \tag{17}$$

where the subscript w and o designate water and oil, respectively.

The unconsolidated media used in this investigation consisted of materials having a structure relatively stable in the presence of the hydrocarbon liquid. Although a large number of materials were investigated in preliminary stages of the investigation, a complete set of data was obtained on only five of the unconsolidated media. These media, however, represented a very wide range of hydraulic characteristics. A description of the five materials on which more or less complete data were obtained is as follows:

1. Volcanic sand--This material comes from a wind-blown deposit along Crab Creek in Washington State. It consists of dark-colored aggregates which can be broken down into finer particles by pressure. It is not known to what degree these aggregates are themselves permeable, but they undoubtedly have some permeability. At any rate, this sand has a degree of structure and has both primary and secondary porosity.

2. Fine sand--This sand was supplied by the Hanford Laboratories of General Electric Company at Richland, Washington, and apparently contains some volcanic minerals. It contains a wide range of particle sizes, ranging down to silt size. Most of the particles are angular and not as rounded as most river bed sands.

3. Glass beads--The beads were purchased from the Minnesota Mining and Manufacturing Company and designated as size 130-5005. This material is an example of media having a very narrow range of pore sizes. It is not much different in this respect, however, from many clean river bed sands.

4. Fragmented mixture--This medium was obtained by mixing aggregates created by crushing oven-dried clay and a consolidated sandstone with the volcanic sand. The aggregates were crushed until all passed through a #32 sieve. This material was created to simulate a soil having a well aggregated structure with secondary as well as primary porosity. The aggregates were much more stable, however, than those found in ordinary soils.

5. Touchet silt loam--This soil comes from the Columbia River basin and was also supplied by the Hanford Laboratory. It is extremely fine textured in that it contains practically no coarse sand, but it is somewhat unusual in that it contains a smaller amount of clay than would be expected in such a fine-textured soil. It is, in fact, nearly pure silt mixed with some extremely fine sand. It contains enough clay, however, to create a structure with secondary porosity.

In addition to the five unconsolidated media, two consolidated sandstone cores were investigated. One of these, Berea Sandstone, was cut perpendicular to the bedding planes. In the dry state and in the fully saturated state the stratification was not visible. After saturating the material completely with liquid and then desaturating to a value of S of about 0.80 to 0.90, the strata became plainly visible. At this average saturation, the finer-textured strata were still fully saturated and darker than the partially desaturated coarser-textured strata. The finer and coarser strata alternate in position in a more or less regular pattern, the individual strata being about 1/8 inch thick.

The other sandstone investigated, Hygiene from the Pierre Formation in Colorado, contains no visible bedding. It contains a substantial amount of clay and thus has a rather high value of S_r (0.577). It has an unusually narrow pore-size distribution for a material having such a high residual saturation. The significant hydraulic properties of the seven media described above are tabulated in Tables 1 - 4 in Appendix III.

Because the theory on which equation (15) is based assumes that $K_{rnw} = 1$ at $S = S_r$, K_{nw} is defined in this paper in a somewhat arbitrary manner; i.e., the value of K_{nw} used in the denominator of the ratio K_{rnw} was obtained by extrapolating K_{nw} vs. P_c/γ to large values of P_c/γ. At values of S less than S_r, the values of K_{rnw} may be greater than 1; but since the theory does not apply to this range of saturations, the variation of K_{rnw} in this range was not investigated in detail. Where the data are available, however, they are tabulated in the tables.

Another reason for defining K_{rnw} in this way was that in the case of the unconsolidated media, it was not practical to determine the actual maximum

---

* Soltrol "C" core test fluid. Phillips Petroleum Company, Special Products Division, Bartlesville, Oklahoma.

air permeability, K_{nw}. It was possible to determine the air permeability before the media were saturated in the air permeability cell, but this was usually not the maximum value of air permeability as determined after the samples had been vacuum saturated and then desaturated. This value of K_{nw} often exceeded the air permeability value of dry media even before S was reduced to S_r. Evidently, the process of saturating and then drying caused the pulling together of fine material into aggregates and the creation of larger pores.

The samples could not be brought to a satura-tion of S_r in a reasonable time by increasing the negative pressure of the outflow tube. They could, of course, have been dried further by evaporation, but this would have foiled the material balance calculation of the saturation. Experiments with unconsolidated media were actually terminated at $S > S_r$. The samples were removed from the cell and the volume of of liquid remaining in the sample was measured gravimetrically. This volume of liquid was added to the volume removed during the experiment to obtain the volume at a saturation of 1.0 so that material balance computations of saturations at other values of P_c/γ could be made.

The first step in checking the theory represented by equations (13), (14), (15), and (16) was the determination of the parameters P_b and λ from the data shown in figure 1. The data were replotted as figure 2 in which S_e is shown as a function of P_c/γ. These curves were obtained after successive approximations of the residual saturation S_r as described in Appendix II.

The negative of the slope of the straight line portion of a curve, e.g., those shown in figure 2, is designated as λ and is called the "pore-size distribution index". The extrapolation of the straight line to the ordinate representing $S_e = 1.0$ gives the value of the parameter P_b which is called the "bubbling pressure". This particular value of capillary pressure is called bubbling pressure because it was found experimentally that for homogeneous and isotropic media, it is very close to the capillary pressure at which the first gas flow can be observed. The bubbling pressure apparently represents the smallest capillary pressure at which a continuous gas phase exists. At smaller values of P_c, the theory does not appear to be valid for either the wetting or the nonwetting permeabilities.

Having determined the parameters P_b and λ, equation (16) was solved to obtain relative permeabilities to air as a function of P_c/γ. The solutions of equation (16) are shown in figure 5 as solid lines. The data points represent measured values. It can be seen from the figures that the measured values of air relative permeability are in reasonably close agreement with the theoretical curves in every case except for the Berea Sandstone. Undoubtedly the failure of the theory in the latter case is a result of the anisotropy of this medium. Because air flow across bedding planes is restricted by the layers having the highest individual bubbling pressures, the measured values of K_{rnw} are less than the theoretical values at corresponding values of P_c. This phenomenon has been described elsewhere by Corey and Rathjens [7].

In the case of the unconsolidated media, the experimental procedure provided no direct comparison of measured values of K_{rw} with theoretical curves of K_{rw} as a function of P_c. This was because the theoretical curves were computed from the parameters λ and P_b which were obtained in a separate experiment. In general, the packing and the resultant values of ϕ and P_b/γ are difficult to reproduce with precision, especially in a totally different kind of container.

Figure 6, however, shows measured values of K_{rw} as a function of P_c/γ. The solid curves are computed from equation (14) using values of λ and P_b/γ obtained with the air permeability cell. In most cases the agreement between measured and com-

puted values of K_{rw} is good. In the case of the Touchet silt loam, the computed curve is displaced toward higher values of P_c/γ at corresponding values of K_{rw}. In the case of the Fragmented Mixture, it is displaced slightly toward lower values of P_c/γ.

Evidently, in the case of the Touchet silt loam, the pressurized sleeve of the air permeability cell caused this soil to be compressed more (and thus have smaller pores) than was the case for the same soil when packed by the automatic packer in the rigid columns used for the K_{rw} measurements.

It is noteworthy, however, that the slopes of the measured curves on the log-log plot of K_{rw} as a function of P_c/γ are essentially the same as for the calculated curves. In other words, the measured values of η are in close agreement with the relationship $\eta = 2 + 3\lambda$ even though λ was determined in a separate experiment. Evidently, the pore-size distribution index is less sensitive to packing differences than are the values of ϕ and P_b.

For the consolidated sandstone, the agreement with respect to both P_b and λ is excellent as is shown in curves 2 and 3 on figure 6b. The anisotropy of Berea Sandstone has a less noticeable effect on K_{rw} than on K_{rnw}.

A comparison of measured values of K_{rnw} as a function of S with theoretical curves is shown in figure 7 for unconsolidated media. The theoretical curves were computed from equation (15). The agreement between measured and computed values of K_{rnw} is reasonably close. There is, however, a tendency for the measured values of K_{rnw} to be displaced toward smaller values than the predicted curves at the mid-range of S.

The authors suspect that the reason for this displacement is a result of a failure of the theory caused by the assumption that K_{enw} is a maximum at $S = S_r$ and that $K_{rnw} = 1$ at $S = S_r$. As previously explained, a value of K_{nw} was chosen so that measured values of K_{rnw} would extrapolate to a value of 1 at S_r. The measured curve, therefore, is fitted to the theoretical curve at this point. It would be possible to choose a value of K_{nw} such that the measured curve would fit the theory at the midpoint. In this case the measured values would cross the theoretical curve.

It might be possible in the future to perfect the theory in such a way as to account for the fact that K_{enw} is not a maximum at S_r but this remains to be done.

It is also possible that the results shown in figure 7 are affected by a failure to achieve complete
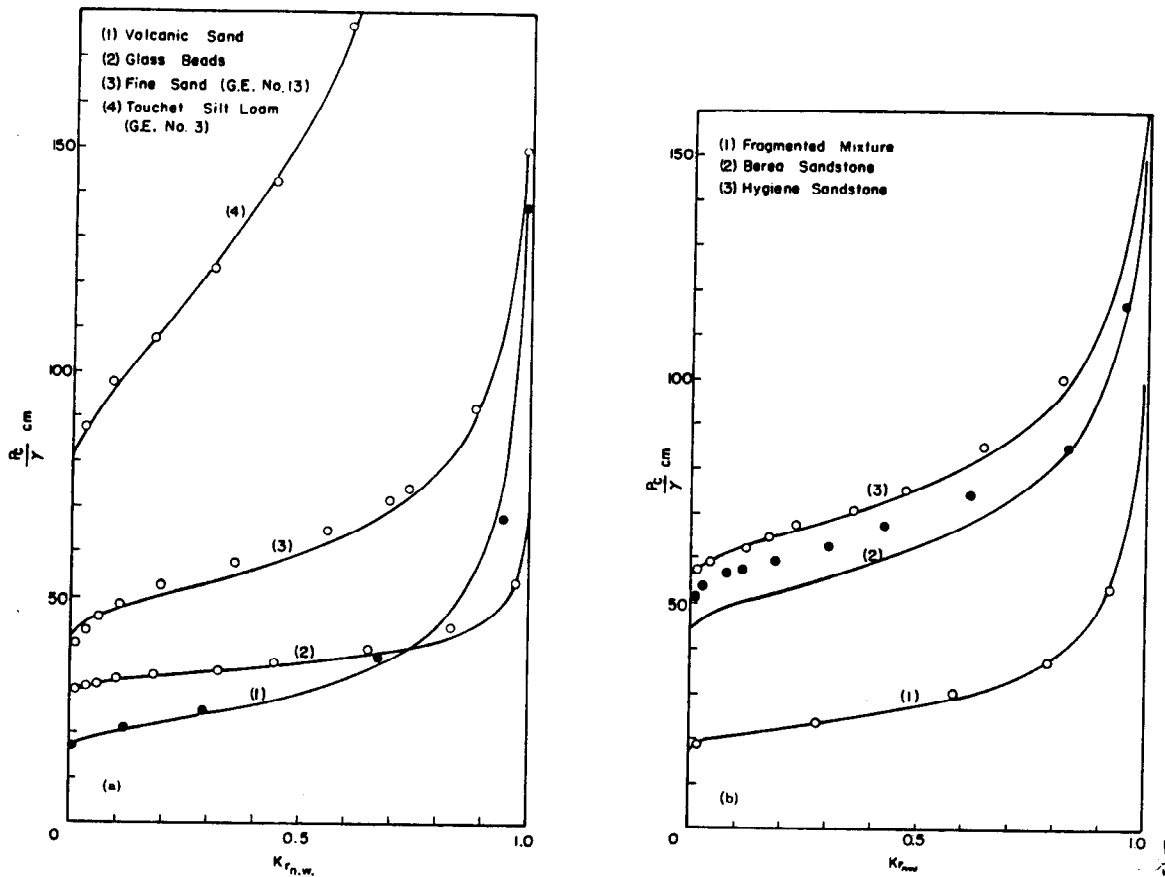
Figure 5. Theoretical curves and experimental data of capillary pressure head as a function of nonwetting phase relative permeability.
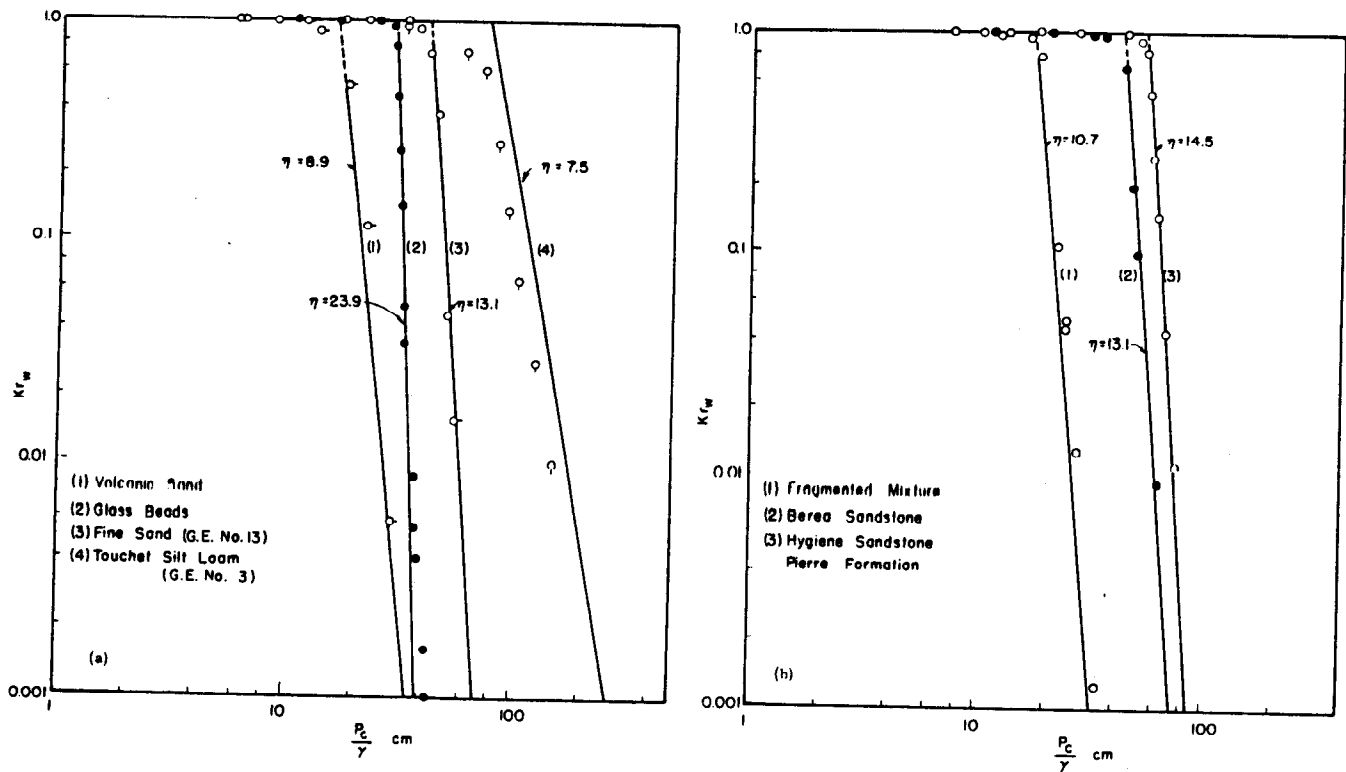
Figure 6. Predicted wetting phase relative permeability as a function of capillary pressure head compared with experimental data.
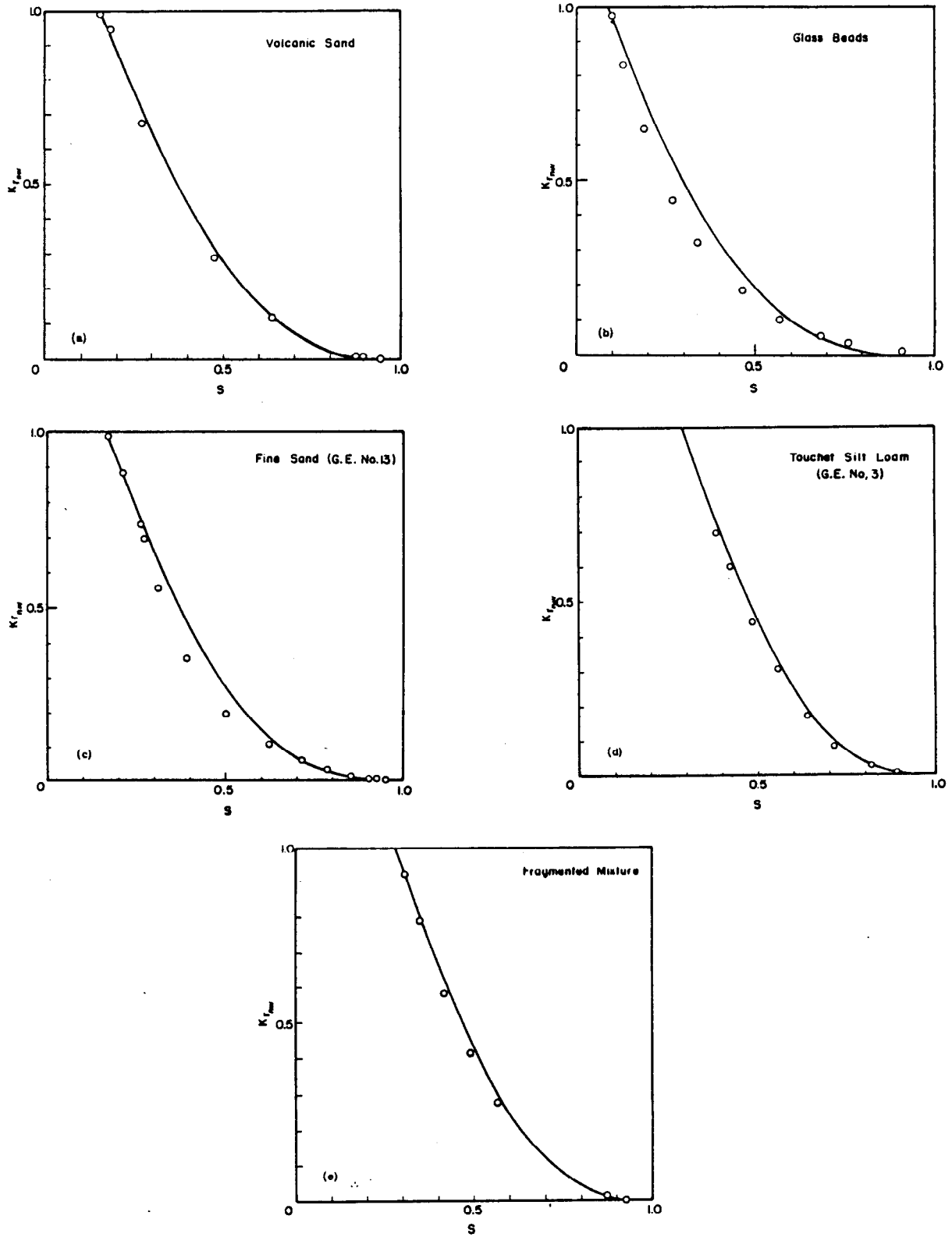
Figure 7. Theoretical curves and experimental data of nonwetting phase relative permeability as a function of saturation for unconsolidated porous materials.
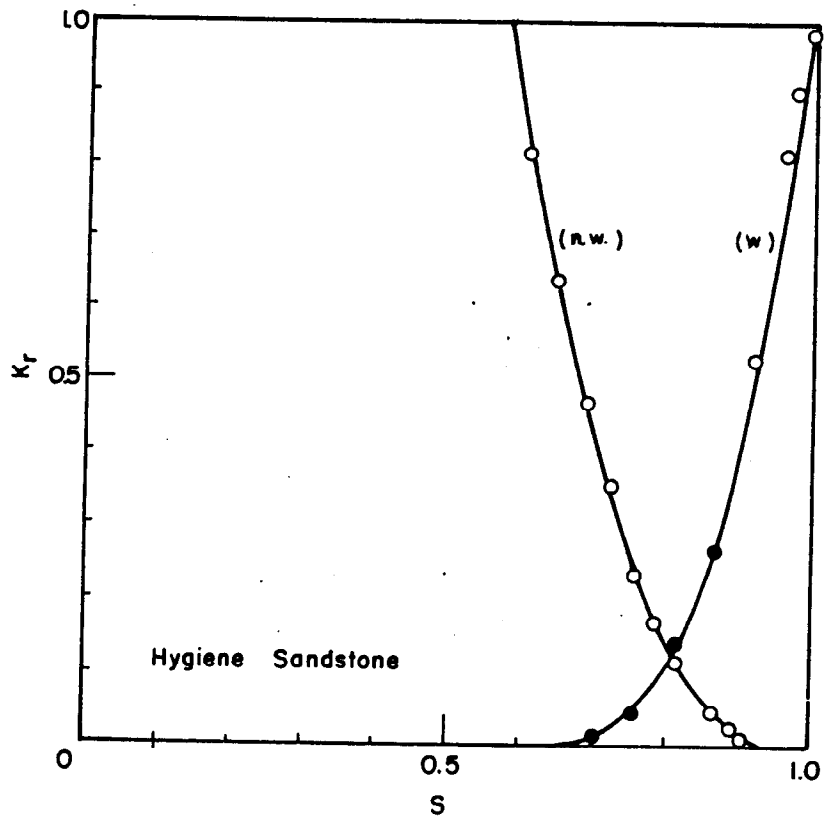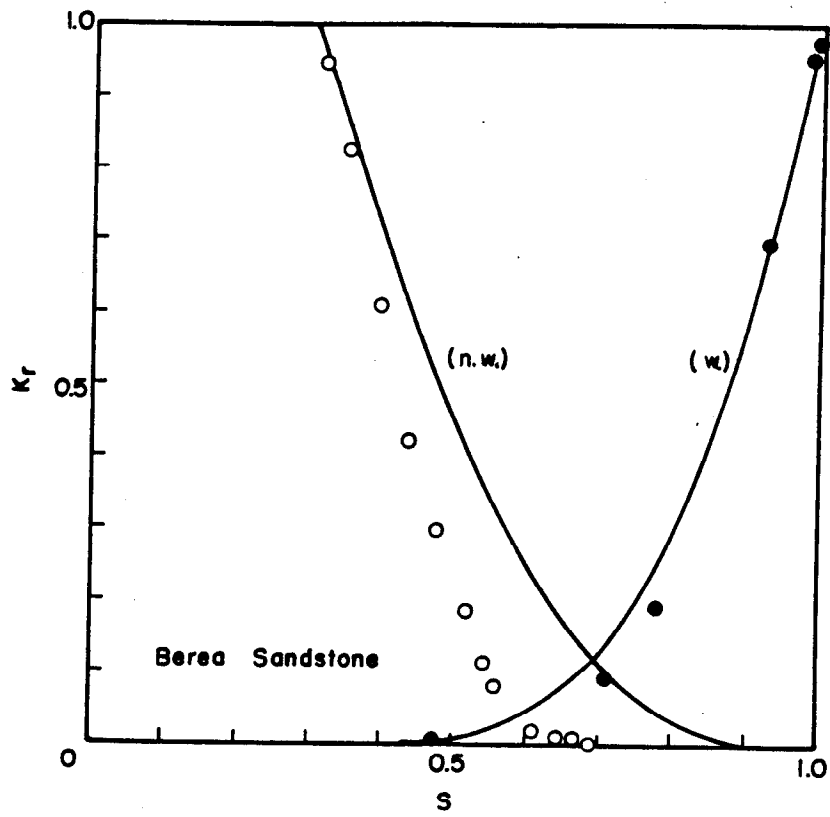
Figure 8. Theoretical curves and experimental data for relative
permeabilities of the nonwetting (nw) and wetting (w) phases
as a function of saturation for two consolidated sandstones.

isotropy and to eliminate boundary effects entirely in the air permeability cell.

It is practically certain that boundary conditions did affect the measurement of K_w in the column permeameters used for unconsolidated media. This is evident because the value of K_w was often higher than the maximum values of K_{nw} measured in the air permeameter even when the porosity of the medium was the same. If the reverse had been true, the result could have been attributed to gas slippage. But the higher value of K_w can only be attributed to a lesser resistance along the boundary in the rigid column as compared to the cell with the pressurized sleeve.

An unrealistically high value of K_w should not affect the measured values of η but would affect the absolute values of K_{rw} .

In the case of the consolidated sandstones, it was possible to check equations (13), (14), (15), and (16) on exactly the same medium because in this case there was no chance of a change in $P_c/\gamma = f(S)$ for the two experiments. The results are shown in figure 8. The measurements, in the case of the Hygiene Sandstone, are in nearly perfect agreement with the theory for both the nonwetting and wetting relative permeability curves.

For Berea Sandstone, however, the values of K_{rnw} are much smaller than predicted. They are, in fact, zero at values of S corresponding to capillary pressures much larger than the predicted

bubbling pressure. This is undoubtedly a result of anisotropy since finer-textured layers block the flow of air.

Evidently, the K_{rw} curves are much less sensitive to this kind of anisotropy because the K_{rw} curve is in reasonably close agreement with the predicted curve.

It will be noted from figure 2 that materials with secondary porosity have smaller values of λ (and thus smaller values of η) than materials without secondary porosity. This can be seen most distinctly by the contrast in the slope of the curve for volcanic sand and that for glass beads shown in figure 2. The practical significance of this phenomenon is discussed in the section to follow.

The authors have made measurements of K_{rw} as a function of P_c/γ for one sample of fragmented clay (see Table #2--Fragmented Lamberg Clay, Appendix III) which has a value of η of 3.6, indicating a value of λ of 0.53. They have also computed values of η from capillary pressure versus saturation curves which were only slightly greater than 2.0, the theoretical lower limit.[*] The lowest predicted values of η were obtained on samples of very fine-grained consolidated rocks containing much clay but having some larger pores because of cracks and vugular spaces.

---

[*] Unpublished private report: "Evaluation of Capillary-Pressure Field Data" by A. T. Corey. Petroleum Research Corp., Denver, Colorado.

Miller and Miller [13] have described the requirements for similitude of isotropic porous systems containing two immiscible fluid phases (air and water) in which the air pressure is considered to be constant but both air and water are continuous phases. In this case, flow of only the liquid phase is considered.

The same assumptions made by Miller and Miller are accepted in the following analysis. This analysis is in many respects the same as theirs but it is restricted to the drainage cycle in order to avoid the complication of hysteresis. In addition, the theoretical functional relationships among P_c, S_e, K_{rw}, and K_{rnw} are used to simplify the resulting expressions for the criteria of similitude.

An equation describing the flow and macroscopic distribution of the liquid is derived by combining Darcy's law with the equation of continuity applicable to flow in porous media. The continuity equation is

$$\text{div } q = -\phi_e \frac{\partial S_e}{\partial t} \tag{18}$$

where ϕ_e is the "effective porosity". The effective porosity is similar if not identical to the "drainable porosity" commonly employed by drainage engineers and is used here in order to be consistent with the use of the effective saturation S_e. The effective porosity, ϕ_e, is related to ϕ by the relation:

$$\phi_e = (1 - S_r) \phi \tag{19}$$

The result of combining Darcy's law with equation (18) is

$$\text{div}\left[\frac{\gamma K_e}{\mu} \nabla\left(\frac{P}{\gamma} + Z\right)\right] = \phi_e \frac{\partial S_e}{\partial t} \tag{20}$$

which is essentially the equation first derived by L. A. Richards [17].

Equation (20) is next written in a dimensionless form by scaling the variables appearing in the equation. The variables can be scaled by choosing standard units of permeability, length, pressure and time which are known to be significant characteristics of the system. The standard units are designated as K_o, L_o, P_o, and t_o respectively. The standard unit K_o is simply the fully saturated (maximum) permeability K of the medium under consideration. Using the standard units as scaling factors, equation (20) becomes

$$\frac{t_o K_o \gamma}{L_o \mu \phi_e} \text{ Div.}\left[K_r \nabla \cdot \left(\frac{P}{P_o} + \frac{Z\gamma}{P_o}\right)\right] = \frac{\partial S_e}{\partial(t/t_o)} \tag{21}$$

where the dots after the divergence and gradient operator symbols indicate that the operations are performed with respect to scaled coordinate lengths.

Equation (21) can be simplified by choosing appropriate system parameters as the standard

units P_o, L_o, and t_o. An obvious choice for P_o is the bubbling pressure P_b. If P_b is chosen as the standard unit of pressure, it is necessary to use P_b/γ as the standard unit of length. Similarly, the appropriate standard unit of time is $\phi_e P_b \mu / K\gamma^2$. Scaled variables of pressure, length, and time are obtained by dividing the unscaled variables by their respective standard units.

Substituting the standard units into equation (21) gives

$$\text{Div. }[K_r \nabla \cdot (P. + Z.)] = \frac{\partial S_e}{\partial t.} \tag{22}$$

where the dots designate scaled variables or operators with respect to scaled variables.

Equation (22) will yield identical particular solutions in terms of scaled variables provided that:

1. Geometric similitude exists.

2. The boundary and initial conditions in terms of scaled variables are identical.

3. The functional relationships among K_r, S_e, and P_c/P_b are identical for both systems.

The macroscopic boundary conditions can be identical only if corresponding lengths which are characteristic of the macroscopic size of the system are identical multiples of the length P_b/γ. If two systems are geometrically similar in a macroscopic sense, it is necessary to choose only one characteristic length "L" and the size requirement is satisfied if the ratio $P_b/\gamma L$ is identical for any two systems under consideration.

From the theory and experimental verification presented in the preceding sections, it is evident that the last requirement is satisfied if the pore-size distribution indexes λ are identical. It will be noted that λ is a function of the microscopic geometry of the porous media. Use of λ as a criterion of similitude eliminates the need for explicit consideration of other microscopic geometric variables such as were suggested by Miller and Miller [13]. Furthermore, P_b is a function not only of the size of the pores but also of the interfacial forces, contact angle, shape, etc. Use of P_b/γ as a unit of length eliminates the necessity of explicit consideration of the similitude with respect to these variables.

The foregoing analysis indicates that a valid model involving flow of liquid in a partially saturated porous medium requires the following:

1. The medium must have the same pore-size distribution index, λ.

2. The macroscopic boundaries of the model must have a shape and orientation similar to the prototype.

3. The size of the model must be such that $\gamma L/P_b$ is the same as for the prototype.

4. The initial conditions in terms of scaled time, i.e., $t K \gamma^2/P_b \mu \phi_e$ must be the same for model as for the prototype.

If the prototype involves steady state flow only, the last of these requirements can be eliminated. If the saturation in any part of a system increases as well as decreases with time, it is possible that additional requirements may enter. It is possible, also, that if the system contains a discontinuous gas phase, the requirements listed may not be sufficient for similitude, especially if a region of increasing liquid saturation exists.

There is a possibility, however, that even when hysteresis is a factor, λ may be sufficient to describe the pertinent microscopic geometric properties. This possibility is discussed in the section dealing with hysteresis.

One difficult aspect of creating a valid model is finding a porous medium having the appropriate value of λ and at the same time having a sufficiently small value of P_b/γ such that the model can be of a practical size. It is easy to find coarse sands or gravels having a small value of P_b/γ but as indicated earlier and as discussed by Rahman [15], these will have a narrow range of pore sizes (large λ) regardless of the range of grain sizes used. Unfortunately, most prototype media of engineering interest have smaller values of λ. One possibility of overcoming this difficulty would be the use of stable aggregates such as crushed sandstone or naturally occurring volcanic soil.

As can be seen from the values of λ tabulated in Appendix III (Table 2), these materials have pore-size distribution indexes in the same range as soil with structure. They can have, moreover, values of P_b as small as desired.

It should be noted that equation (20) could have been written in terms of S and ϕ, rather than S_r and ϕ_e. If the variables are expressed in terms of S and ϕ, however, the parameter S_r becomes an explicit rather than an implicit factor in similitude. The curves of K_r and K_{rnw} as a function of S as well as ϕ for the model would have to be identical to those for the prototype. Use of the variables S_e and ϕ_e reduce the difficulty of meeting the similitude requirements. It is easier to find media having similar functional relationships between relative permeability and S_e than between relative permeability and S because S_r is eliminated as a factor affecting the shape of the curves. Expressing the liquid content of the media as a percentage of dry weight or a percentage of bulk volume makes the requirements even more difficult to satisfy than the use of S.

A model designed in accordance with the theory presented here must be restricted in its application to systems that do not reach saturations less than S_r because the theory is applicable only to saturations greater than S_r.

If the problem under investigation is not explicitly concerned with the conditions in the partially saturated zone, the pertinent characteristics of the behavior of the system may not be extremely sensitive to λ. This might be true, for example, if the partially saturated zone is very narrow compared to the fully saturated zone. In the latter case, it might be possible to ignore λ in choosing a medium for a model, but it would still be necessary to consider $P_b/\gamma L$.

When conditions in the partially saturated zone are of explicit concern, it is not possible to ignore λ. In the latter case, glass beads or clean sands are not suitable materials for modeling systems involving flow in soils with structure. This is clear from the results shown in the preceding section.

For a further discussion of the practical significance of the parameters P_b/γ and λ, specifically in the field of drainage engineering, the reader is referred to a paper by the authors [2] dealing with this subject.

The preceding discussion has dealt almost entirely with systems in which it is assumed that the saturation of the medium either remains constant or decreases with time. Systems involving an increasing liquid saturation are of equal engineering importance. Unfortunately, the functional relationships among P_c , S , K_{rw} , and K_{rnw} are usually not the same on a cycle of increasing S as on a cycle of decreasing S . The reason for this has been discussed by Miller and Miller [13].

A question that needs to be answered is whether the criteria of similitude suggested in the preceding section are sufficient when hysteresis may be involved. In order to gain some insight into this problem, the authors made an investigation of K_{rw} as a function of P_c on the imbibition as well as the drainage cycle. One of the coauthor's students, Larry G. King, has made many measurements of K_{rw} as a function of P_c on the imbibition cycle for his doctorate thesis [10] which is concerned with imbibition. An example of his data is presented in figure 9.

A detailed description of how these data were obtained is given in the thesis by King. Briefly, a soil column similar to those used by the authors was initially packed with dry soil. Relative liquid permeabilities as a function of capillary pressure first were obtained on the imbibition cycle until the saturation apparently reached a maximum. The measurements were then obtained as the column was drained. Afterwards, the column was vacuum-saturated and measurements were made as the column was drained from the completely saturated state. In other experiments, King first vacuum saturated the column and after making measurements on the drainage cycle resaturated the column by imbibition.

There are several noteworthy observations that can be made from King's data, i.e.,

1. The slope of the curves of K_{rw} as a func-

tion of P_c are practically the same for both the drainage and imbibition cycle.

2. When a medium is resaturated or drained from a state which is neither completely dry nor fully saturated with liquid, the curves do not follow an intermediate path between the drainage or imbibition curves. Instead (after a short transition) the curves jump from one to the other of the two possible paths.

3. The values of K_{ew} on the imbibition cycle tend to approach a maximum of about 0.45 - 0.50 of that obtained when the medium is vacuum saturated. At this state, the nonwetting phase is air, and it is apparently able to diffuse away with time. The authors have observed a slow increase in K_{ew} with time at a constant value of P_c , the rate of increase being more rapid for fine material than for sands. In time, the media become full saturated with liquid by imbibition.

4. At values of $P_c > P_b$, the permeabilities on the drainage cycle are a minimum of one order of magnitude greater than on the imbibition cycle.

From the foregoing observations it would seem that a possibility does exist that the criteria of similitude presented in the preceding section will sometimes be adequate for systems involving hysteresis. At least, this may be true for systems not involving a discontinuous gaseous phase. The possibility will be greatly enhanced if it can be shown that a definite relationship exists among λ , P_b , and the ratio of the permeability on the drainage cycle to that on the imbibition cycle at particular values of P_c . Such a relationship, however, remains to be demonstrated.
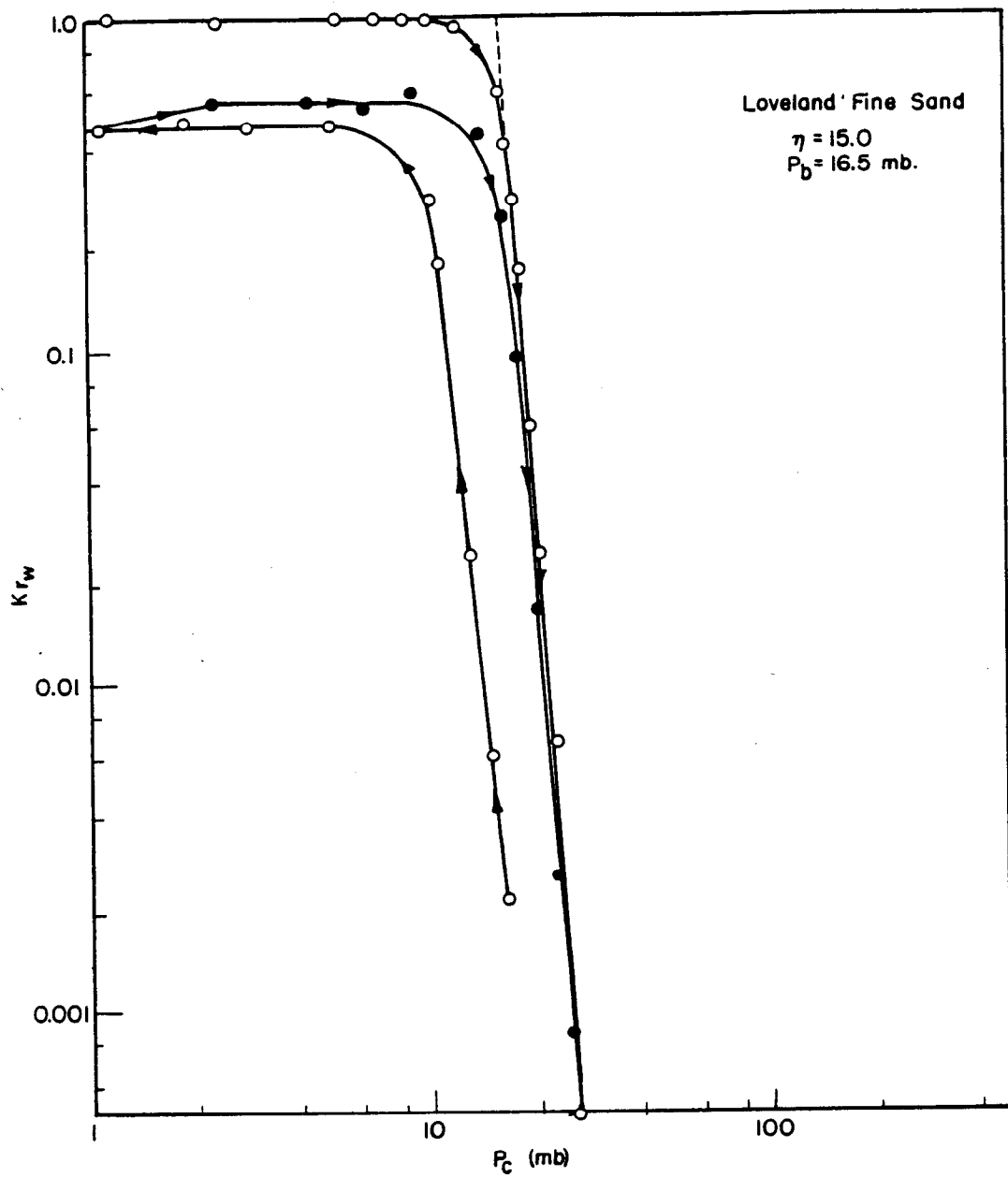
Figure 9. Wetting phase relative permeability as a function of capillary pressure on the imbibition and drainage cycles.

REFERENCES

1. Averjanov, S. F., About permeability of subsurface soils in case of incomplete saturation. Engineering Collection Vol. VII, 1950, as quoted by P. Ya. Polubarinova Kochina; The Theory of Ground Water Movement. English translation by J. M. Roger DeWiest, 1962, Princeton University Press.

2. Brooks, R. H. and Corey, A. T., Hydraulic properties of porous media and their relation to drainage design, submitted for publication in ASAE transactions.

3. Burdine, N. T., Relative permeability calculations from pore-size distribution data. Trans. AIME, 1952.

4. Carman, P. C., Fluid flow through granular beds. Trans. Inst. Chem. Eng. (London) Vol. 15, 1937.

5. Corey, A. T., The interrelation between gas and oil relative permeabilities. Producer's Monthly, Vol. XIX, No. 1, Nov., 1954.

6. Corey, A. T., Measurement of water and air permeability in unsaturated soil. Soil Science Society of America Proceedings, Vol. 21, No. 1 January-February, 1957.

7. Corey, A. T. and Rathjens, C. H., Effect of stratification on relative permeability. Tech. Note No. 393, Journal of Petroleum Technology, December, 1956.

8. Irmay, S. On the hydraulic conductivity of unsaturated soils. Trans., AGU, Vol. 35, No. 3, June, 1954, p. 463-67.

9. Jackson, R. D., Reginato, R. J.; and Reeves, W. E.; A mechanized device for packing soil columns. U. S. D. A., ARS 41-52, April, 1962.

10. King, L. G., Imbibition of fluids by porous media. A Ph. D. thesis in process, Colorado State University.

11. Kozeny, J., Stz. ber. Akad. Wiss. Wien, Abt. IIa, 136, 1927, as quoted in reference 17.

12. Loomis, A. G., and Crowell, D. C., Relative permeability studies: 1. Gas-oil systems. Producer's Monthly, Vol. 22, No. 11, Sept., 1958.

13. Miller, E. E., and Miller, R. D., Physical theory for capillary flow phenomena. J. Appl. Physics, Vol. 27, 1956.

14. Naar, J. and Wygal, R. J, Structure and properties of unconsolidated aggregates. A manuscript supplied by the Gulf Research and Development Company and submitted for publication to Trans. of the Faraday Society, April 17, 1962.

15. Rahman, Q. H., Permeability and capillary pressure in sands. A masters thesis submitted to the SEATO Graduate School of Engineering, Bangkok, Thailand, 1961.

16. Reeve, R. C., and Brooks, R. H., Equipment for subsampling and packing fragmental soil samples for air and water permeability tests. Soil Sci. Society of Amer. Proc., Vol. 17, 1953.

17. Richards, L. A., Capillary conduction of liquids through porous mediums, Physics 1, 1931.

18. Scott, V. H., and Corey, A. T., Pressure distribution during steady flow in unsaturated sands. Soil Science Society of America Proceedings, Vol. 25, No. 4, July-August, 1961.

19. Wyllie, M. R. J. and Gardner, G. H. F. The generalized Kozeny-Carman Equation. World Oil, March and April, 1958.

20. Wyllie, M. R. J. and Spangler, M. B. Application of electrical resistivity measurements to problem of fluid flow in porous media. Bulletin of the American Association of Petroleum Geologists, Vol. 36, No. 2, February, 1952.

The Theoretical Basis for the Burdine Equations

The theory presented below is a variation of theory published in petroleum engineering literature [3, 5, 19, 20]*. It is realized that most irrigation and drainage engineers do not have easy access to this literature. This synopsis is included here, therefore, for the convenience of the readers.

The assumption is made that fluid compressibility and inertia are not significant factors affecting the flow so that the equation of Navier-Stokes reduces to a statement that the gradient of piezometric pressure P* is balanced by the viscous drag. For a Newtonian viscous fluid, this relationship is given by

$$\underline{\nabla} P^* = \mu \nabla^2 \underline{V} \tag{1}$$

where $\underline{V}$ is the total velocity vector. Equation (1) can be solved for particular boundary conditions, e. g., 1-dimensional flow through straight tubes, flow between infinite flat parallel plates, and film flow over an infinite flat plate. The solution of equation (1) for each of these particular boundary conditions will be presented to show how the solutions vary with the shape of the boundary.

Flow through a small diameter tube is considered first. For this geometry it is more convenient to express the quantity $\nabla^2 \underline{V}$ in cylindrical coordinates, i.e.,

$$\underline{\nabla}P^* = \mu \left[\frac{1}{r} \frac{\partial}{\partial r}\left(r \frac{\partial V}{\partial r}\right) + \frac{\partial}{\partial \theta}\left(\frac{1}{r}\frac{\partial V}{\partial \theta}\right) + \frac{\partial}{\partial x}\left(r \frac{\partial V}{\partial x}\right) \right]. \tag{2}$$

where r is measured from the centerline of the tube toward the boundary. If the flow is steady, there is no variation in $\underline{V}$ along the tube in the direction x. The last term on the right of equation (2) is, therefore, zero. Because of symmetry, the term involving $\frac{\partial V}{\partial \theta}$ is also zero so that finally

$$\underline{\nabla}P^* = \mu \left[\frac{1}{r} \frac{d}{dr}\left(r \frac{du}{dr}\right) \right] \tag{3}$$

where u is the component of velocity along the tube. Because the flow is laminar, there is no component of $\underline{V}$ perpendicular to x .

Since there is no flow perpendicular to the boundary, ∇P^* likewise has no component perpendicular to the boundary. This implies that the equipotential lines are planes perpendicular to the axis of the tube. The gradient of P* , therefore, does not depend on r and can be treated as a constant. The variables, u and r , are separable and after integrating once, the relationship

$$\frac{r^2}{2\mu}\nabla P^* = r \frac{du}{dr} + C \tag{4}$$

is obtained. In order for equation (4) to be valid at the centerline where r = 0, the value of C is zero since $\frac{du}{dr}$ cannot be infinitely large. Therefore,

$$\frac{r}{2\mu} \nabla P^* = \frac{du}{dr} \quad . \tag{5}$$

After separating the variables, integrating and using the condition that $\frac{du}{dr}$ is finite (which implies the velocity of the fluid approaches the velocity of the boundary at the boundary) then

$$u = \frac{\nabla P^*}{4\mu} (r_t^2 - r^2) \tag{6}$$

where r_t is the radius of the tube.

Integrating the discharge over the entire cross-sectional area of a tube of radius r_t and dividing by the cross-sectional area gives the equation of Poiseuille for the mean velocity, i.e.,

$$\bar{u} = - \frac{r_t^2}{8\mu} \nabla P^* \tag{7}$$

Solving equation (1) for 1-dimensional flow in a flow in a film over a flat plate gives

$$\bar{u} = - \frac{d^2}{3\mu} \nabla P^* \tag{8}$$

where d is the thickness of the film. Similarly,

$$\bar{u} = - \frac{b^2}{12\mu} \nabla P^* \tag{9}$$

for 1-dimensional flow between parallel flat plates where b is the spacing of the plates.

It will be noted that equations (7), (8), and (9) are of a similar form in that u is proportional to ∇P^*, and to the square of a length dimension characterizing the size of the flow section. The volume flux is inversely proportional to viscosity and a numerical constant.

By induction, then, an analagous equation applying to straight tubes of uniform cross section of any shape is

$$\bar{u} = - \frac{R^2}{k\mu} \nabla P^* \tag{10}$$

where R is a length characterizing the size of the tube, and k is a numerical constant depending on the shape of the cross section and the dimension chosen to characterize the size.

In applying equation (10) to tubes of irregular shape, the question arises as to what length dimension should be used to characterize the size of the tubes. One possibility is the hydraulic radius, R . It is defined as the cross-sectional area divided by the wetted perimeter.

If equations (7), (8), and (9) are rewritten in terms of R , only the numerical constant is changed. Poiseuille's equation becomes

$$\bar{u} = - \frac{R^2}{2\mu} \nabla P^* \tag{11}$$

and equations (8) and (9) become

$$\bar{u} = - \frac{R^2}{3\mu} \nabla P^* \quad . \tag{12}$$

---

* References are given at the end of the body of the publication.

The variation in the constant k is evidently, greatly reduced.

It is reasonable to suppose that (from a hydrodynamic viewpoint) flow in a thin film is about as different from flow in a circular tube as it is possible to obtain. One might conclude, therefore, that the shape factor for irregular cross sections (e.g. the pore space in a porous solid) should be somewhere between 2 and 3. This conclusion would not be valid, however, if the cross section has an extreme "eccentricity". Consider, for example, a cross section as shown in Figure 1. Note that the perimeter of the

Figure 1. An Example of a Tube Cross-Section with Extreme Eccentricity.

long extension of the cross section is great but the area is small and the contribution to flow of this part of the area is, relatively, even smaller.

The difficulty is that the distribution of velocity in one part of the cross section is like that in a relatively large tube whereas in the extension, it is like that between closely spaced plates. The large part of the eccentric cross section, therefore, would act as a tube with $k \approx 2$ whereas the extension would act as a tube with $k \approx 3$. The larger part, however, has a much larger hydraulic radius than the extension. Note that in equation (10), R is squared and k is to the first power. One cannot, therefore, use R for the entire cross section and an average of k to obtain a valid estimate of $\bar{u}$.

It is much more reasonable to regard the eccentric cross section shown in figure 1 as two separate cross sections. The error resulting from applying an average k of about 2.5 for each cross-section will not be great, but it is necessary to use separate values of R. An alternative method (which will give exactly the same result) is to consider the entire cross section as a whole, using an average k and a mean value of R^2, designated as $\overline{R^2}$.

The tubes considered in developing equation (10) were straight. There is no difficulty in extending the analysis to other than straight tubes provided that the actual length of the tubes can be measured and the direction that any fluid element is moving at any particular location is known. There is an error in such an analysis if the normal acceleration resulting from flow around bends is disregarded. This error is small, however, if the tangential velocity is very small.

If it is desired to determine $\bar{u}$ as a function of the potential difference between the ends of a tortuous tube and the direct distance between the two ends, the tortuosity will have two effects. The first effect is with respect to $\bar{u}$. If the direction between the two ends of the tube is defined as the x direction, then $\bar{u}$ varies from point to point because the direction of the axis of the tube varies, i.e., the component of velocity in the x direction varies even though the magnitude of the velocity remains constant. If $|\underline{v}|$ is the magnitude of the average tangential velocity, the mean value

of the x component is given by

$$\bar{u} = |\underline{v}| \frac{L}{L_e} \qquad (13)$$

where L is the direct distance between the ends of the tube and L_e is the length of the tortuous tube. The quantity $|\underline{v}|$ in equation (13) is analagous to $\bar{u}$ in equation (10).

The second effect of the tortuosity of the tube is with respect to $\nabla P *$. If it is desired to express the driving force as $\frac{\nabla P *}{L}$, it must be noted that

$$\left|\overline{\nabla P *}\right| = \frac{\nabla P *}{L}\left(\frac{L}{L_e}\right) \qquad (14)$$

where $\left|\overline{\nabla P *}\right|$ is the absolute value of the mean gradient of $P*$. An equation relating $\bar{u}$ to $\frac{\nabla P *}{L}$ in a tortuous tube (analagous to equation 10) is, therefore, given by

$$\bar{u} = -\frac{\overline{R^2}}{k\mu(L_e/L)^2}\frac{\nabla P *}{L} \qquad (15)$$

where the quantity $\left(\frac{L_e}{L}\right)^2$ has been called <u>tortuosity</u> and designated by the symbol T.

It is evident that for porous solids of a given porosity the greater the eccentricity of the pore space, the larger will be $\overline{R^2}$. This is equivalent to saying that $\overline{R^2}$ will be greater for porous solids, having secondary porosity as well as primary porosity, other things being equal. This can be visualized most easily by considering a porous solid containing an abundance of clay. If somehow all of the solid matter could be concentrated into one solid portion of the cross section and the remaining section was free to conduct fluids, the value of K would obviously be much greater than if the clay particles were evenly distributed over the cross section.

Futhermore, the value of $\overline{R^2}$ for the non-wetting phase, on the other hand will increase as the saturation increases. The relationship between $\overline{R^2}$ for the wetting phase and S can be deduced from a curve of S as a function of P_c; e.g. as shown in figure 1 of the text.

The principle is based on the assumption that a connected cross section of an irregular-shaped tube can be regarded as composed of a large number of sub-sections each having a discrete R. The values of R^2 of each sub-section are summed and the mean value of R^2 is obtained. The entire pore space filled with the wetting phase is then regarded as a single tube of irregular shape (but uniform cross-sectional area) having an average shape factor k and mean value of hydraulic radius $\overline{R^2}$.

Another key assumption of this theory is that to a close approximation,

$$P_c dA = \sigma d(wp) \cos\theta \qquad (16)$$

where P_c is the capillary pressure at a particular

saturation S, dA is the area of the portion of the cross section of the pore space that would desaturate if S undergoes a change dS at the capillary pressure P_c, $d(wp)$ is the corresponding change in perimeter of the desaturated area at the soil-wetting phase interface, and θ is the angle of contact of the wetting phase at the solid interface. It is further assumed that θ and σ remain constant over the range of saturations considered.

The hydraulic radius of the area dA is, therefore, given by

$$R = \frac{dA}{d(wp)} = \frac{\sigma \cos \theta}{P_c} \quad . \tag{17}$$

The mean value of R^2 for the wetting phase at the saturation S (designated as $\overline{R_w^2}$) is given by

$$\overline{R_w^2} = \frac{\sigma^2 \cos^2 \theta}{S} \int_0^S \frac{dS}{P_c^2} \quad ; \tag{18}$$

similarly, for the non-wetting phase,

$$\overline{R_{nw}^2} = \frac{\sigma^2 \cos^2 \theta}{1 - S} \int_S^1 \frac{dS}{P_c^2} \quad . \tag{19}$$

Although the integral in equation (18) is over the interval of S from 0 to S, for practical purposes it could often just as well be taken over the interval from S_r to S. The value of the integral from 0 to S_r is very small because P_c is very large over this region.

According to Carman [4], the tortuosity of fully saturated porous solids which are isotropic and granular in nature is about 2. Other kinds of porous media may have other values of tortuosity. If, for example, the medium is composed of clay particles oriented perpendicular to the direction of flow, T will be much larger than 2. If the clay is oriented parallel to the flow, T will be smaller than 2.

The variation of tortuosity with S was studied experimentally by Burdine [3] and later analytically by Wyllie and Gardner [19]. Burdine obtained an empirical expression for $T(S)$ in the form

$$\left[\frac{T_{1.0}}{T_S} \right]_w = \left[\frac{S - S_r}{1 - S_r} \right]^2 \tag{20}$$

where the subscript w indicates that the relationship applies to the wetting phase. In other words, the quantity $\frac{1}{T_c}$ varies linearly from zero at $S = S_r$ to 1.0 at $S = 1.0$. This finding was verified by Corey [5] and was later derived by Wyllie and Gardner [19] using a mathematical model of porous solids somewhat different from the model employed here.

The corresponding relationship found by Burdine for the nonwetting phase is

$$\left[\frac{T_{1.0}}{T_S} \right]_{nw} = \left[1 - \frac{S - S_r}{S_c - S_r} \right]^2 \tag{21}$$

where S_c is called the "critical saturation". At $S > S_c$, the nonwetting phase is discontinuous. Corey [5] found for isotropic media that replacing S_c by 1.0 did not materially change the calculated permeabilities for saturations less than S_c.

The volume flux, q, in a porous medium of having a porosity ϕ is related to the velocity $\overline{u}$ in the pores by $q = \overline{u} \phi S$. Thus equation (15) becomes

$$q = \frac{\phi S \overline{R^2}}{k \mu T^2} \frac{\nabla P^*}{L} \quad . \tag{22}$$

Noting the similarity between equation (22) and Darcy's Law, it would seem that

$$K_{ew} = \frac{\phi S \overline{R_w^2}(S)}{k T_w^2(S)} \tag{23}$$

in which it is assumed that ϕ and k are independent of S. Assuming that $\overline{R_w^2}(S)$ and $T_w(S)$ are as given by equations (18) and (20) respectively, the equation for the relative permeability of the wetting phase is given by

$$K_{nw} = \left[\frac{S - S_r}{1 - S_r} \right]^2 \frac{\int_0^S \frac{dS}{P_c^2}}{\int_0^1 \frac{dS}{P_c^2}} \quad ; \tag{24}$$

similarly, for the nonwetting phase,

$$K_{rnw} = \left[1 - \frac{S - S_r}{S_c - S_r} \right]^2 \frac{\int_S^1 \frac{dS}{P_c^2}}{\int_0^1 \frac{dS}{P_c^2}} \tag{25}$$

Equations (24) and (25) are known as Burdine's equations for relative permeability.

In Burdine's equations, the parameters σ^2, $\cos^2 \theta$, k, and ϕ cancel. It is possible therefore, that the theory with respect to relative permeability is more precise than with respect to permeability, per se.

It is certainly true that Burdine's theory is of more practical use in determining the dependence of relative permeability on saturation than it is for determining permeabilities. The permeabilities of porous media when occupied fully by only one fluid are easily measured directly. The direct measurement of relative permeability curves is a much more difficult and time-consuming process.

Burdine's equations, however, are applicable only for fairly isotropic media as one would suspect from the manner of their derivation. Anisotropy causes marked departures from the isotropic case as has been described by Corey and Rathjens [7]. The effect of anisotropy depends upon the orientation of the discontinuities in texture. Bedding planes perpendicular to flow tend to decrease the maximum saturation S_c at which the nonwetting phase will flow, and bedding planes parallel to flow tend to increase S_c. Such planes also cause inflection in both K_{nw} and K_{rnw} curves.

Method of Determining Residual Saturation

To determine the pore-size distribution index, λ , it is necessary to plot $\log S_e$ versus $\log P_c$ which necessitates determining the residual saturation S_r . Since the saturation, S , is related to S_e by the relation

$$S_e = \frac{S - S_r}{1 - S_r} \quad \text{for } S_r < S \leq 1.0 \tag{1}$$

it is necessary to have measured values of S as a function of P_c/γ to determine S_r .

An approximate value of S_r is obtained by selecting a value of S at which the curve of P_c/γ versus S appears to approach a vertical asymtote as shown in figure 1. With this estimate of S_r , tentative values of $\log S_e$ are computed and plotted as a function of $\log P_c/\gamma$. Usually, the plot will not be a straight line, but an intermediate portion of the computed values will fall on a straight line as shown in figure 2.

A second estimate of S_r is then obtained such that a value of S_e , in the high capillary pressure range which does not lie on the straight line, will fall on the straight line as shown in figure 2. The second estimate of S_r is usually adequate, and all of the points will lie sufficiently close to a straight line when the points are recomputed using the new value of S_r . If this is not the case, the process is repeated until a value of S_r is obtained that results in a straight line for most values of $P_c/\gamma > P_b/\gamma$.

At large values of P_c/γ where the curve becomes asymtotic to some value of S , S_e is very sensitive to the value of S_r chosen, i.e., a small change in S_r makes the change in S_e look big on a log-log plot. Therefore, values of S_e at this end of the curve that do not lie exactly on the straight line should not be given much consideration in selecting a value of S_r .
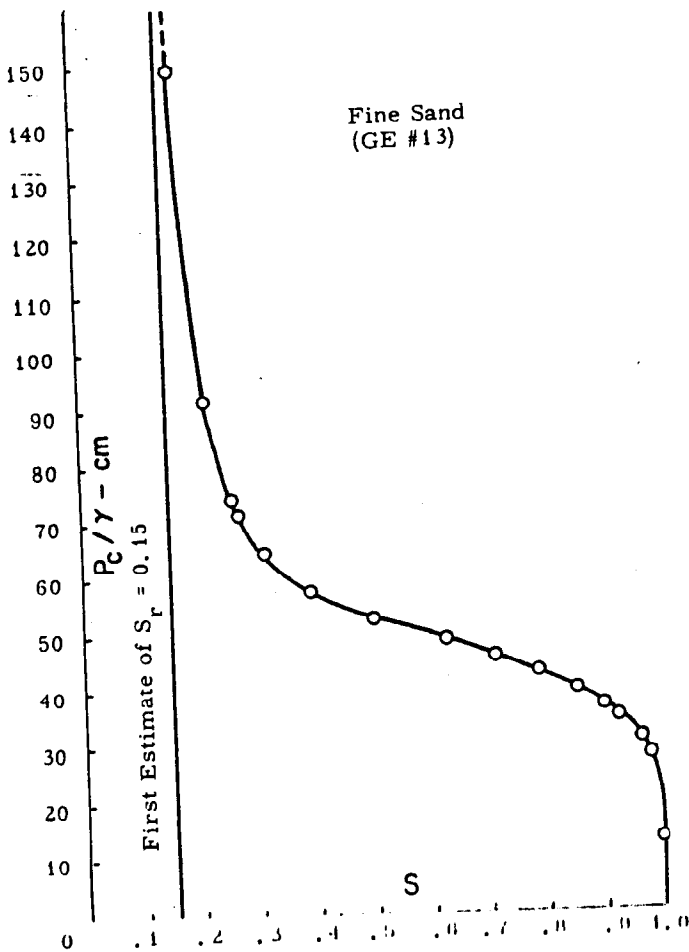

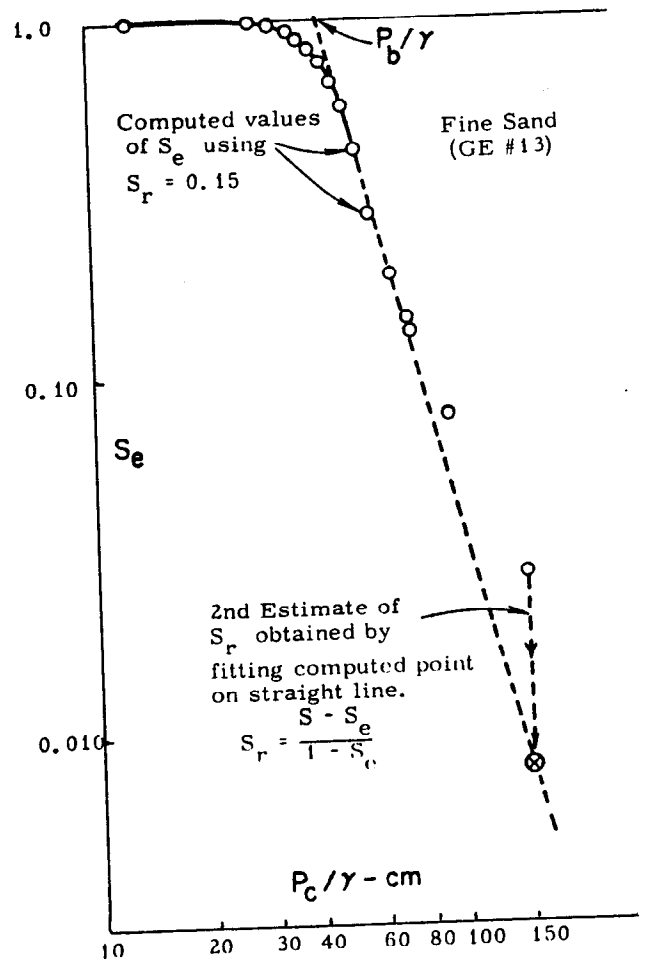Fig. 1 Capillary pressure head as a function of saturation

Fig. 2 Effective saturation as a function of capillary pressure head

TABLE 1

Data from Air Permeability Cell
for Unconsolidated Samples

Volcanic Sand

$\phi = 0.351$ $P_b/\gamma = 16.0$ cm.
$K_{nw} = 18.0\,\mu^2$ $S_r = 0.157$
$\lambda = 2.29$ $\phi_e = 0.296$

P_c/γ (cm.)	S	K_{enw} (μ^2)	K_{rnw}
6.9	1.00		
8.6	1.00		
10.5	1.00		
12.0	0.990		
13.5	0.986		
14.5	0.980		
15.5	0.974		
16.0	0.948	0.0112	0.00062
17.0	0.895	0.0720	0.0040
17.2	0.875	0.123	0.0068
21.0	0.638	2.10	0.117
24.8	0.479	5.20	0.289
36.9	0.277	12.1	0.672
67.7	0.188	17.0	0.944
136.6	0.158	17.8	0.990

Fine Sand (G. E. #13)

$\phi = 0.377$ $P_b/\gamma = 41.0$ cm.
$K_{nw} = 2.5\,\mu^2$ $S_r = 0.167$
$\lambda = 3.7$ $\phi_e = 0.314$

P_c/γ (cm.)	S	K_{enw} (μ^2)	K_{rnw}
12.8	0.990		
27.8	0.980		
30.8	0.962		
31.8	0.950	0.00234	0.000935
34.8	0.926	0.00700	0.00280
36.8	0.901	0.0115	0.00460
39.8	0.855	0.0298	0.0119
42.8	0.788	0.0808	0.032
45.8	0.716	0.150	0.060
48.8	0.627	0.259	0.104
52.8	0.503	0.486	0.194
57.7	0.393	0.886	0.354
64.8	0.314	1.39	0.556
71.7	0.273	1.74	0.696
74.4	0.262	1.84	0.735
92.1	0.217	2.20	0.880
150.1	0.174	2.47	0.989

Fragmented Mixture (granulated clay + fragmented sandstone + volcanic sand)

$\phi = 0.443$ $P_b/\gamma = 17.2$ cm.
$K_{nw} = 11.3\,\mu^2$ $S_r = 0.276$
$\lambda = 2.89$ $\phi_e = 0.321$

P_c/γ (cm.)	S	K_{enw} (μ^2)	K_{rnw}
10.9	0.991		
13.0	0.978		
14.1	0.969		
15.0	0.962		
16.0	0.951		
17.0	0.924	0.021	0.00182
18.4	0.871	0.173	0.0150
23.6	0.562	3.14	0.278
30.5	0.415	6.56	0.581
37.7	0.348	8.90	0.788
53.7	0.303	10.4	0.920

Glass Beads ("3M" #130-5005)

$\phi = 0.370$ $P_b/\gamma = 29.0$ cm.
$K_{nw} = 6.30\,\mu^2$ $S_r = 0.085$
$\lambda = 7.3$ $\phi_e = 0.338$

P_c/γ (cm.)	S	K_{enw} (μ^2)	K_{rnw}
3.8	1.00		
5.9	0.995		
11.8	0.989		
17.8	0.985		
23.8	0.980		
26.9	0.971		
28.8	0.938	0.022	0.00152
29.1	0.912	0.090	0.00360
30.4	0.764	0.209	0.0332
31.0	0.681	0.352	0.056
32.1	0.579	0.630	0.100
32.7	0.465	1.140	0.181
33.9	0.337	2.03	0.322
35.7	0.269	2.79	0.443
39.0	0.190	4.09	0.649
43.8	0.130	5.24	0.831
53.5	0.099	6.15	0.976
150.4	0.097	6.26	0.995

Touchet Silt Loam (G. E. # 3)

$\phi = 0.485$ $P_b/\gamma = 75.0$ cm.
$K_{nw} = 0.60\,\mu^2$ $S_r = 0.270$
$\lambda = 1.82$ $\phi_e = 0.349$

P_c/γ (cm.)	S	K_{enw} (μ^2)	K_{rnw}
7.8	1.00		
12.8	1.00		
17.8	1.00		
22.8	1.00		
32.8	0.998		
42.8	0.995		
52.8	0.992		
62.8	0.984		
67.8	0.978		
72.5	0.967		
77.8	0.946	0.00360	0.00060
82.3	0.892	0.0069	0.00115
87.7	0.821	0.0157	0.0262
97.8	0.719	0.0506	0.0844
107.6	0.641	0.105	0.175
123.0	0.562	0.185	0.308
142.6	0.492	0.264	0.440
177.0	0.424	0.359	0.600
207.2	0.383	0.418	0.695

Fragmented Fox Hill (1) Sandstone

$\phi = 0.47$ $P_b/\gamma = 10.3$
$K_{nw} = 30.0\,\mu^2$ $S_r = 0.30$
$\lambda = 1.92$ $\phi_e = 0.329$

P_c/γ (cm.)	S	K_{enw} (μ^2)	K_{rnw}
3.9	1.00		
5.9	1.00		
7.6	0.972		
8.7	0.956	0.0144	0.000480
10.0	0.860	0.600	0.0200
12.4	0.776	3.20	0.107
15.1	0.663	4.80	0.163
17.8	0.554	9.20	0.305
21.5	0.465	15.7	0.523
25.6	0.416	20.0	0.667
28.9	0.397	22.0	0.734
33.8	0.375	23.4	0.780
46.6	0.339	25.4	0.846
58.0	0.331	27.0	0.900

TABLE 2

Data from Liquid Permeameter Columns for Unconsolidated Samples

Volcanic Sand

$\phi = 0.365$ $P_b/\gamma = 16.8$ cm.
$K_w = 11.0\ \mu^2$ $\eta = 9.0$

P_c/γ (cm.)	K_{ew} (μ^2)	K_{rw}	S
6.3	11.0	1.00	
8.8	11.0	1.00	
11.9	10.75	0.980	
13.3	9.75	0.885	
18.0	5.56	0.506	
22.2	1.26	0.114	
29.7	0.064	0.0058	
40.0	0.00545	0.00050	

Fine Sand (G. E. #13)

$\phi = 0.360$ $P_b/\gamma = 41.0$ cm.
$K_w = 2.85\ \mu^2$ $\eta = 14.6$

P_c/γ (cm.)	K_{ew} (μ^2)	K_{rw}	S
17.3	2.85	1.00	
22.0	2.85	1.00	
25.2	2.85	1.00	
32.9	2.85	1.00	
36.9	2.62	0.92	
41.6	2.03	0.713	
44.7	1.075	0.378	
50.9	0.128	0.045	
54.9	0.0434	0.0152	0.334

Touchet Silt Loam (G. E. #3)

$\phi = 0.469$ $P_b/\gamma = 64.0$ cm.
$K_w = 0.500\ \mu^2$ $\eta = 5.6$

P_c/γ (cm.)	K_{ew} (μ^2)	K_{rw}	S
6.10	0.500	1.00	
6.20	0.497	1.00	
32.2	0.470	0.940	
60.0	0.364	0.728	
72.1	0.298	0.595	
83.9	0.138	0.276	
92.9	0.069	0.138	
103.7	0.0325	0.065	
124.4	0.014	0.028	
149.4	0.0050	0.010	

Glass Beads ("3M" #130-5505)

$\phi = .383$ $P_b/\gamma = 29$ cm.
$K_w = 10.5\ \mu^2$ $\eta = 20$

P_c/γ (cm.)	K_{ew} (μ^2)	K_{rw}	S
10.7	10.4	1.00	
16.4	10.4	1.00	
24.8	10.6	1.00	
28.1	9.94	0.945	
29.0	8.08	0.770	
30.0	4.80	0.457	
30.5	2.67	0.254	
31.2	1.485	0.141	
32.8	0.523	0.0498	
32.9	0.363	0.0346	
37.1	0.0925	0.0088	
37.2	0.057	0.0054	
38.6	0.042	0.0040	
42.6	0.0170	0.0016	
43.0	0.0104	0.0010	0.117

Fragmented Mixture (granulated clay + fragmented sandstone + volcanic sand)

$\phi = .441$ $P_b/\gamma = 18.5$ cm.
$K_w = 15.0\ \mu^2$ $\eta = 10.9$

P_c/γ (cm.)	K_{ew} (μ^2)	K_{rw}	S
7.6	15.0	1.00	
10.2	14.9	0.993	
12.3	14.75	0.983	
16.6	14.2	0.946	
18.7	11.8	0.786	
22.4	1.56	0.104	
24.3	0.721	0.048	
24.2	0.672	0.045	
27.5	0.189	0.0125	
34.2	0.0191	0.00127	0.376

Fragmented Fox Hill (2) Sandstone

$\phi = 0.503$ $P_b/\gamma = 20.5$ cm.
$K_w = 16.1\ \mu^2$ $\eta = 9.3$

P_c/γ (cm.)	K_w (μ^2)	K_{rw}	S
7.85	16.1	1.0	
11.3	16.1	1.0	
13.8	15.55	0.967	
15.4	13.1	0.815	
17.7	11.7	0.728	
22.2	7.74	0.48	
27.2	1.68	0.104	
31.0	0.32	0.021	
37.5	0.057	0.0036	
43.1	0.0187	0.0012	0.358

Fragmented Lamberg Clay

$K_w = 2.2\ \mu^2$ $P_b/\gamma = 17.5$ cm.
$\eta = 3.6$

P_c/γ (cm.)	K_{ew} (μ^2)	K_{rw}	S
4.50	2.20	1.00	
7.02	2.11	0.96	
18.10	1.225	0.544	
37.4	0.142	0.0645	
38.5	0.130	0.0590	
60.5	0.0145	0.007	

Sand (G. E. #2)

$K_w = 3.05\ \mu^2$ $P_b/\gamma = 38$ cm.
$\eta = 10.0$

P_c/γ (cm.)	K_{ew} (μ^2)	K_{rw}	S
4.8	3.05	1.000	
14.6	3.03	0.993	
21.9	2.39	0.784	
28.8	2.14	0.705	
37.1	1.385	0.454	
42.9	0.783	0.257	
46.6	0.430	0.141	
51.1	0.160	0.0525	
60.5	0.0334	0.01095	

Sand (USSL #3445)

$K_w = 1.48\ \mu^2$ $P_b/\gamma = 43$ cm.
$\eta = 10.1$

P_c/γ (cm.)	K_{ew} (μ^2)	K_{rw}	S
29.2	1.480	1.00	
43.6	1.100	0.743	
52.4	0.218	0.147	
66.2	0.0188	0.0127	
87.0	0.0184	0.0124	
73.6	0.0072	0.0049	

TABLE 3

Data from Liquid Permeameter for

Consolidated Rock Cores

Berea Sandstone (Core perpendicular to bedding planes)				Hygiene Sandstone from Pierre formation (No visible bedding planes)			
$\phi = 0.206$		$P_b/\gamma = 42.0$ cm.		$\phi = 0.250$		$P_b/\gamma = 54.0$ cm.	
$K_w = 0.481\ \mu^2$		$\eta = 11.1$		$K_w = 0.178\ \mu^2$		$\eta = 14.1$	
P_c/γ (cm.)	S	K_{ew} (μ^2)	K_{rnw}	P_c/γ (cm.)	S	K_{ew} (μ^2)	K_{rnw}
11.5	1.00	0.484	1.00	13.3	1.00	0.178	1.00
20.5	1.00	0.481	1.00	18.4	1.00	0.178	1.00
31.9	0.990	0.469	0.976	27.4	1.00	0.177	1.00
35.9	0.985	0.458	0.955	44.9	0.995	0.175	0.985
43.7	0.926	0.333	0.695	51.3	0.975	0.161	0.904
48.0	0.778	0.095	0.197	54.1	0.960	0.135	0.814
50.2	0.706	0.0475	0.0990	56.6	0.920	0.0950	0.530
62.4	0.476	0.00450	0.00930	59.3	0.865	0.047	0.265
88.4	0.345			62.1	0.817	0.026	0.144
116.9	0.313			67.7	0.756	0.0077	0.043
				75.1	0.690	0.0020	0.0110
				85.2	0.643		
				100.6	0.604		

TABLE 4

Data from Air Permeameter for

Consolidated Rock Cores

Berea Sandstone (Core cut perpendicular to visible bedding planes)				Hygiene Sandstone from Pierre Formation (No visible bedding planes)			
$\phi = 0.206$		$P_b/\gamma = 43$ cm.		$\phi = 0.250$		$P_b/\gamma = 54$ cm.	
$K_{nw} = 0.348\ \mu^2$		$S_r = 0.299$		$K_{nw} = 0.128\ \mu^2$		$S_r = 0.577$	
$\lambda = 3.69$		$\phi_e = 0.144$		$\lambda = 4.17$		$\phi_e = 0.106$	
P_c/γ (cm.)	S	K_{enw} (μ^2)	K_{rnw}	P_c/γ (cm.)	S	K_{enw} (μ^2)	K_{rnw}
dry	0.00	0.496	1.42	dry	0.000	0.171	
51.0	0.687	0.00190	0.00545	57.0	0.905	0.00126	0.00985
51.5	0.663	0.00352	0.0101	57.8	0.890	0.00300	0.0234
52.4	0.643	0.00437	0.0126	59.0	0.865	0.00580	0.0453
54.0	0.610	0.00825	0.0237	62.0	0.813	0.0150	0.117
56.6	0.556	0.0284	0.0816	64.4	0.785	0.0217	0.169
57.5	0.540	0.0407	0.117	67.5	0.757	0.0294	0.230
59.3	0.513	0.0648	0.186	70.8	0.723	0.0450	0.352
62.5	0.473	0.104	0.299	75.1	0.690	0.0600	0.469
67.5	0.434	0.148	0.425	85.2	0.643	0.0820	0.640
74.3	0.392	0.213	0.611	100.6	0.604	0.104	0.813
85.0	0.350	0.287	0.825				
117.0	0.318	0.330	0.948				
	0.244	0.425	1.22				
	0.175	0.469	1.35				

27

PREVIOUSLY PUBLISHED PAPERS

Colorado State University Hydrology Papers

No. 1. "Fluctuations of Wet and Dry Years, Part I, Research Data Assembly and Mathematical Models," by Vujica M. Yevdjevich, July 1963.

No. 2. "Evaluation of Solar Beam Irradiation as a Climatic Parameter of Mountain Watersheds," by Richard Lee, August 1963.

Colorado State University Fluid Mechanics Papers

No. 1. "A Resistance Thermometer for Transient Temperature Measurements," by J. L. Chao and V. A. Sandborn, March 1964.

No. 2. "Measurement of Turbulence in Water by Electrokinetic Transducers," by J. E. Cermak and L. V. Baldwin, April 1964.